공학박사 학위논문

A Study on Risk-based Layout Optimization for Sustainable Chemical Process Design

지속 가능한 화학 공정 설계를 위한 리스크 기반의 배치 최적화에 관한 연구

2013년 8월

서울대학교 대학원

화학생물공학부

한 규 상

Abstract

A Study on Risk-based Layout Optimization for Sustainable Chemical Process Design

Kyusang Han
School of Chemical and Biological Engineering
The Graduate School
Seoul National University

This thesis presents the method and applications of process layout optimization based on the quantitative assessment of the individual risk (IR) in order to limit the effect to humans from the accidents can occur in a chemical process. The process layout of chemical plants is usually designed in a compact configuration for economic efficiency, although most of the chemical process units operate under high pressure and temperature, and/or deal with hazardous materials which are flammable or toxic. The possibility of the accident such as fires, explosions, and toxic gas releases which can cause severe damage to humans and properties is always present,

and the social concerns of the community for this are also accompanied. Therefore, a method to quantitatively evaluate the risks arise from the chemical process equipment/facilities is required so that the actual damage can be prevented. This study tries to achieve such goal by proper arrangement of the process layout.

First, various former approaches for the process layout problem, their formulations, and the solution methods have been analyzed. In addition, the method of quantitative risk assessment (QRA) of chemical processes and the concept of risk indices are introduced.

Subsequently, the formulation of the risk-based layout optimization problem for sustainable chemical process design is presented. The individual risks (IR) caused from the fire and explosion that can affect the workers in the process site and the surrounding public are calculated according to the distance from the equipment, and then converted into the safety distance. The risk zones around the process equipment are modeled by using the safety distance constraints and the former layout optimization problems. Then the costs of process layout including land, pipeline, equipment purchase and protective devices are minimized to determine the economically optimized process layout. The formulation of layout optimization problem uses the framework of mixed-integer linear programming (MILP), and the procedure of iterative search for the

reduced problem is applied to tackle the problem with large scale. Process layout optimization based on individual risk (IR) through these procedures can provide the layout that secures the inherent safety as well as the economic feasibility**.**

The proposed methodology is applied to three kinds of chemical processes for validation. First case is dimethyl ether (DME) filling station; an example of the fuel gas station which is the simplest process but can cause heavy damage to humans due to its typical location. Next application is an ethylene oxide (EO) plant, as an example of general chemical process plant. In that case, the selection among the options for site location with different surrounding land uses is considered. A liquefaction process of an LNG-FPSO (liquefied natural gas - floating production, storage and offloading) vessel is considered last for multi-floor and more space-restricted case. Through these case studies, it has been shown that the proposed method can enhance the sustainability of the process layout by ensuring the safety and support the decision making related to the process layout in the early stage of process design.

Keywords: Chemical process design, Layout optimization, Quantitative risk assessment, Individual risk.

Student Number: 2007-21234

TABLE OF CONTENTS

LIST OF FIGURES

LIST OF TABLES

1 Introduction

Design and operation of a chemical process require great efforts from various fields and they affect the surrounding social communities in many aspects. The conflict between the direction to make such effort to be efficient and the direction to make such impact to be positive is inevitable. The former mainly refers to economic efficiency and the latter includes the safety or environmental friendliness. The concept of sustainability can be a remedy to this situation, and the design of chemical process for the future cannot be done without the consideration of the sustainability. The layout optimization of chemical processes considering safety is one way of such sustainable chemical process design.

As the global competition gets more intensive, many chemical processes employ harsher operating conditions, more dangerous materials, and/or more integrated layout for their efficiency. This might lead the chemical plants to the higher cost competitiveness and productivity, but also can result in the escalated risk from them.

In contrast, there are increasing demands for safe and environment-friendly processes for sustainable development of both chemical plants and related social communities. Many chemical

plants respond to these voices by adopting the safety management systems and reinforced emission regulations. Despite the effort to make chemical processes safe, however, accidents like fires, explosions, and releases of toxic materials are still happening in chemical process plants around the world.

Recent accident cases related to the chemical processes is listed in Table 1.1. These accidents have their own cause of occurrence, but the casualties and the property damage can be mitigated if the proper spacing between the hazardous units and the workspaces or other buildings with population is secured.

In this point of view, the layout of chemical processes should consider the risk from the possible hazards to humans and provide the appropriate measures in advance. This thesis aims to provide the very baseline or guideline to support the decision making concerned with the inherently safe layout of the chemical processes, by formulating and applying the risk-based process layout problem.

Table 1.1 Recent accident cases related to chemical processes

Year	City	Place	Accident type	Casualties
1984	Mexico City, Mexico [1]	LPG terminal	Explosion	650 deaths 6400 injuries
1998	Bucheon, Korea [2]	LPG filling station	Fire and explosion	1 death 96 injuries
2005	Texas, USA [3]	Refinery	Fire and explosion	15 deaths 170 injuries
2012	Gumi, Korea [4]	Chemical company	Toxic release	5 deaths 18 injuries
2013	Texas, USA [5]	Fertilizer plant	Explosion	15 deaths 200 injuries

1.1 Motivation

Usual goal of chemical process layout is economic efficiency. The costs related to the arrangement of process equipment and/or facilities such as pipeline connection cost, land purchase cost, floor construction cost are the targets of minimization [6]. Consequently, the layout results have compact configurations in small process sites.

However, safety, especially the safety for human, is the most important objective for the design of sustainable chemical processes. Although it is not easy to measure the damage to human in monetary unit, a single accident can cause much more cost than the saved from the construction and operation of the process. Therefore, the consideration of safety in the layout optimization of chemical processes is crucial.

Safety for human can be quantitatively estimated as a risk index from quantitative risk assessment (QRA) of chemical processes [7]. Analysis methods for the consequence and frequency of possible accident from chemical process are well-established, and the risk concept is widely used to measure the extent of hazardousness.

Since the risk from a hazard varies with the distance from it, it can be used as a constraint in layout optimization problem. Moreover, there are several recommended criteria of risks for different targets,

so it is possible to apply the risk-based constraints to various subjects. The layout of the chemical processes can be inherently safer if the risk-based constraints are concerned, since the layout optimization is an activity of early stage of chemical process design.

In this context, the series of conversion from the characteristics of hazards of a process to the risk, risk-based blocks, and the proper arrangement of process equipment is the key idea of this study.

1.2 Research scope

This study deals with the optimal layout of facilities or blocks of equipment of chemical processes. For example, equipment and a set of its attachments are regarded as a functional block. Actual arrangement of chemical process equipment requires more detailed work on electrical, mechanical devices and connections such as pipe wrecks.

For risk measurement, several types of fire and explosion are counted. Accident types such as flash fire, pool fire, jet fire, BLEVE (boiling liquid expanding vapor explosion), VCE (vapor cloud explosion) are the most probable cases in chemical processes. Release of toxic materials is only considered in result discussion since the range of risk is much broader for this kind of hazard. The

effects of the consequence of accidents are calculated using the known empirical models rather than the commercial software. The hazard from the pipeline is not included in the risk calculation.

The formulation of layout problem is made in MILP (mixed-integer linear programming) framework, using rectilinear distances between facilities and candidate areas of process site. The shapes of process equipment/facilities and the process site are assumed to be squares or rectangles. The orientation of the process equipment is considered while that of the process site is not.

1.3 Thesis outline

The rest of this thesis consist of four parts: the review of the former research related to this study, the formulation of layout optimization problem based on risk measure, the applications of proposed method to various chemical processes, and the conclusion.

In chapter 2, previous studies and literatures deal with the topics of this thesis are briefly reviewed. Research on layout optimization of chemical processes is analyzed in the view of its origin, various approaches and problem domains, formulations, and applications. Some methodologies of quantitative risk analysis (QRA)

of chemical processes that is considered in this study are also examined.

A new layout optimization approach considering the risk to humans for sustainable chemical process design is proposed in chapter 3. The logical procedure and the mathematical formulation for layout optimization are presented and described.

Chapter 4 presents the applications of the proposed layout optimization framework to three different kinds of chemical processes. The first case is the optimal facility layout of DME (dimethyl ether) filling station considering capacity distribution and surrounding land uses. The arrangement of EO (ethylene oxide) plant is considered next with the site options. Finally, process equipment of liquefaction process of LNG (liquefied natural gas) FPSO (floating production, storage and offloading) is allocated in multiple decks of a vessel.

The last chapter addresses the summary and conclusion of this work, and suggests future research topics from this thesis.

2 Backgrounds Theory

2.1 Process layout optimization

The process layout optimization is a task to allocate and/or arrange the equipment/facilities for sustainability of the process under the given connectivity and land restriction. Since the process units, their connections, and land are the cause of cost, the usual objective function of a layout problem is the minimization of the total cost for the economic efficiency. Other objectives such as operability and flexibility, reliability and safety, and environmental friendliness are also considered for the sustainable chemical process design [6].

minimize	$\sum Cost$
subject to	Connectivity
	Land area

2.1.1 Heuristic models

Through decades, several techniques have been developed for the layout optimization problem. The simple heuristic approach was

introduced first. It was based on the common rules such as the adjacency of units for the similar or related jobs, and the concurrence of processing order and the location of units [8]–[11]. Because the actual process layout problems are too complicated to be solved by this approach, and thus, it cannot provide the optimal solution, it was combined with the Graph theory [12].

In the graph theoretical approaches, the process units and the connection among them are represented as the vertices and edges like in Figure 2.1. The edges have given weights, and the total weight of resulted layout is minimized. Some methods based on the graph theory employ the heuristic layout result as a starting point [13]–[16].

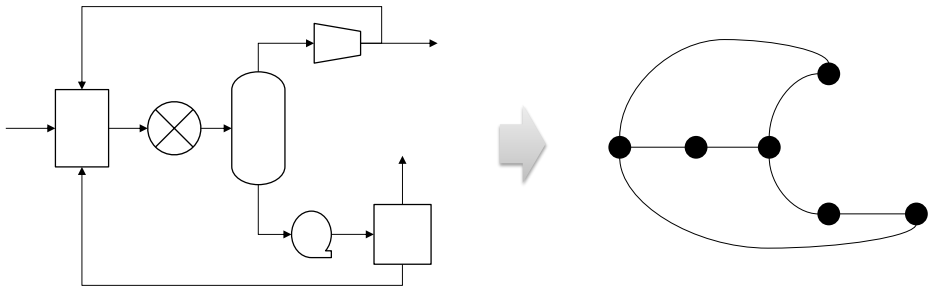

Figure 2.1 An example of graph representation of a process.

2.1.2 Mathematical models

More recently, the major approach in the researches regarding the process layout is mathematical programming techniques [17]–[19]. Several researchers proposed the layout optimization models based on the mixed integer linear programming (MILP) and mixed integer non-linear programming (MINLP).

Some former approaches such as the graph partitioning problem was converted to MILP for solution [14], or other aspects of process design including production scheduling were considered together with the proper layout using mixed integer formulation [20], [21]. Papageorgiou and Rotstein proposed the MILP formulation for the layout optimization in the continuous plane, which became the basis of many other related works including this study [22]. Other applications of layout optimization have their own features: multi-dimensional layout [23]–[25], safety consideration [25], [26], solution efficiency [27], [28], routing of pipes [29], branch-and-bound algorithm [30], etc.

The number of researches using MINLP models is relatively small, but various approaches have been made. After Penteado and Ciric proposed the MINLP model for safe layout considering financial risk [31], the comparison of MILP and MINLP approaches for the block layout design [32], [33], the safe layout under toxic

release scenarios based on the disjunctive programming [34]–[36] for convex hull formulation of non-overlapping constraints [37]–[40], and other approaches have been presented.

The basic difference between these two approaches is the representation of the distance between units: the MILP formulation employs the rectilinear distances, while the Euclidean distances are used in the MINLP models. Figure 2.2 presents the two distance measures.

In regard of this difference, the constraints to prevent the overlapping of units are also different. When a facility is positioned, another facility can be allocated on the left, right, above, or below of it (L, R, A and B in Figure 2.3). To model this situation, many MILP approaches use the big-M constraints with binary variables. However, some MINLP models do not require additional constraints by assuming the size of unit is the footprint size (the dashed circle in Figure 2.2), or use the convex hull approach.

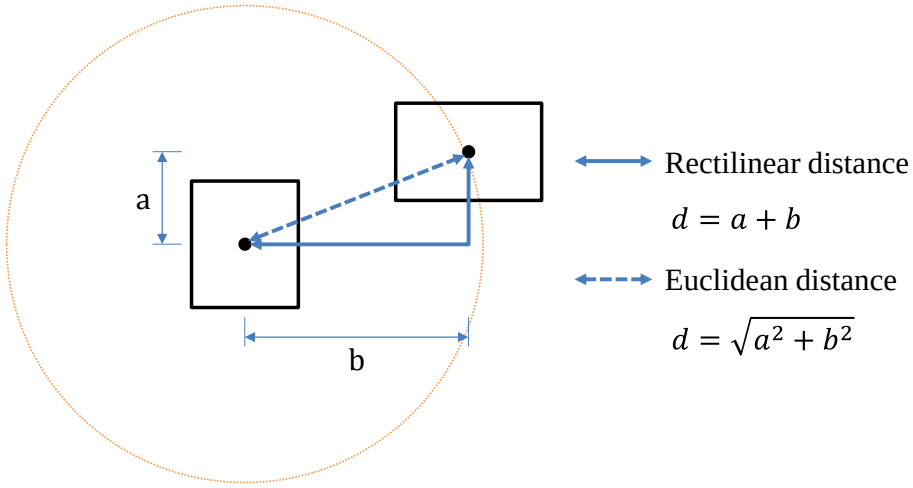

Figure 2.2 Measures of distance between units.

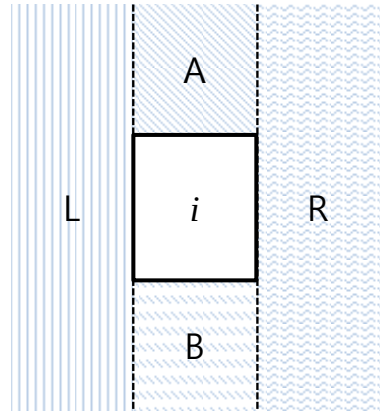

Figure 2.3 Relative positions available to other units without overlap.

Other topics on process layout optimization are the application of stochastic approach, safe layout, and employment of additional information. Stochastic approach [41] to layout problem caught attention in several researches. They used genetic algorithm for the facility layout problems for manufacturing industries [42], [43]–[46]. The safety of layout is considered in many ways. Simple safety distances [47], calculation of possible loss/damage [25], [26], [31] are such examples. Moreover, sustainable layout by adopting the concepts of land use planning [48]–[50], and mapping of risk in resulted process site [51] have been considered recently. The use of external information including geographical data and process knowledge is also a way of improving the layout result [52].

Aforementioned techniques based on the mathematical programming were useful to solve the small-sized layout problems. As the number of the equipment or facilities to be allocated is increased, however, it is very difficult to achieve the optimal solution within the desirable computational effort. For example, the simple MILP approach cannot solve a 12-unit-problem in 10,000 seconds with modern laptop PC [28].

In order to tackle the large-scale layout problems, several approaches for efficient solution have been proposed. The decomposition of the original problem into the master- and sub-

problem [53], the construction-based iteration with initial selection and iterative insertion [27], [54], the tabu search with diversification and intensification procedure [55], and the iterative solutions of reduced problems [28] have been investigated. Although these techniques usually do not guarantee the global optimum, they can solve the layout problem with up to 36 units within hundreds of seconds and provide near-optimal solutions.

2.2 Quantitative risk assessment

2.2.1 Risk indices

A risk index is a comprehensive, integrated representation of accident frequency and consequence. Some indices like Dow's fire and explosion index [56] represent the extent of hazardousness from the possible accidents, while other indices express the possible risk that one can take from the accident: societal risk and individual risk are example of it.

The societal risk is come from the societal concerns due to the dangerous activities such as installation of hazardous chemical facility in/near the social communities. To express the societal risk, the relationship between the number of fatalities (N) and the

frequency (f) or cumulative frequency (F) is considered. That is, the F-N curve is generally used to assess the societal risk [57]–[60].

The individual risk (IR) is an effective measure for quantifying the risk from chemical process equipment to humans, because it is the risk to a person in the vicinity of a hazard and considers the nature, likelihood, and time period of the possible injury to the individual [7].

The basic calculation of risk is usually done by the product of frequency and consequence of accident that came from various quantitative risk analysis methods like Fault Tree Analysis, but IR reflects more elements. To get the IR index, HSE (Health and Safety Executive) suggest a two-step calculation [61]. First, the frequency of fatality (*FoF*) of a person at the location of interest *u*, considering the accident frequency, fatality rate, weather effect, and directional effect is calculated for all the accident scenarios about the event outcome *v*.

$$FoF_u = \sum_v f_{eo,v}\, p_{u,v}^{\mathrm{fat}}\, p_{u,v}^{\mathrm{dir}}\, p_{u,v}^{\mathrm{wea}} \tag{2.1}$$

Then, the fraction of time and probability of the presence of people are multiplied to FoF_u to give IR for the group of people *k* at the location *u*.

$$IR_{u,k} = \theta_k \, p_{u,k}^{\mathrm{loc}} \, FoF_u \tag{2.2}$$

For some accident scenarios such as toxic release, calculation of meteorological condition including wind direction and speed has great importance for risk assessment [37], [39]. In this study, however, this calculation is modified to a simpler one with appropriate assumptions to deal with more general accident cases. We consider the worst-case accident scenario, which means the individual of interest is at the accident location at the time of accident. The meteorological and geographical conditions are also ignored by assuming that the effect of accident to an individual is independent to such factors. Then, individual risk for accident *v* at location *u* becomes the product of two terms.

$$IR_u = \sum_v f_{eo,v} \, p_{u,v}^{\mathrm{fat}} \tag{2.3}$$

Since the IR consist of the accident frequency and fatality rate, the smaller the value of IR, the lower the risk. HSE's framework for the tolerability of risk provides the criteria for the acceptable limits of IR that can be considered as safe [62]. They set up the boundary values of IR between "broadly acceptable", "tolerable", and "unacceptable" levels of risk. For the layout optimization problem of

chemical processes, we use the tolerance limits of IR between tolerable and unacceptable, which are one in a thousand (10^{-3}) per annum for workers and 10^{-4} per annum for the public.

Figure 2.4 illustrates the relationship between the risk triangle concept and the tolerance limit of IR for workers and the public [62]. The possible risks (death rates) in life are overlapped for comparison [63], [64].

The level of risk of process units varies with the distance from them, since the fatality rate is affected by distance from the hazardous equipment [65]. Therefore, the IR tolerance limits mentioned above can be used to determine the minimum separation distances from equipment so the safety of both workers and the public can be secured. The distances satisfying such IR values are implemented as the distance constraint in the layout optimization problem.

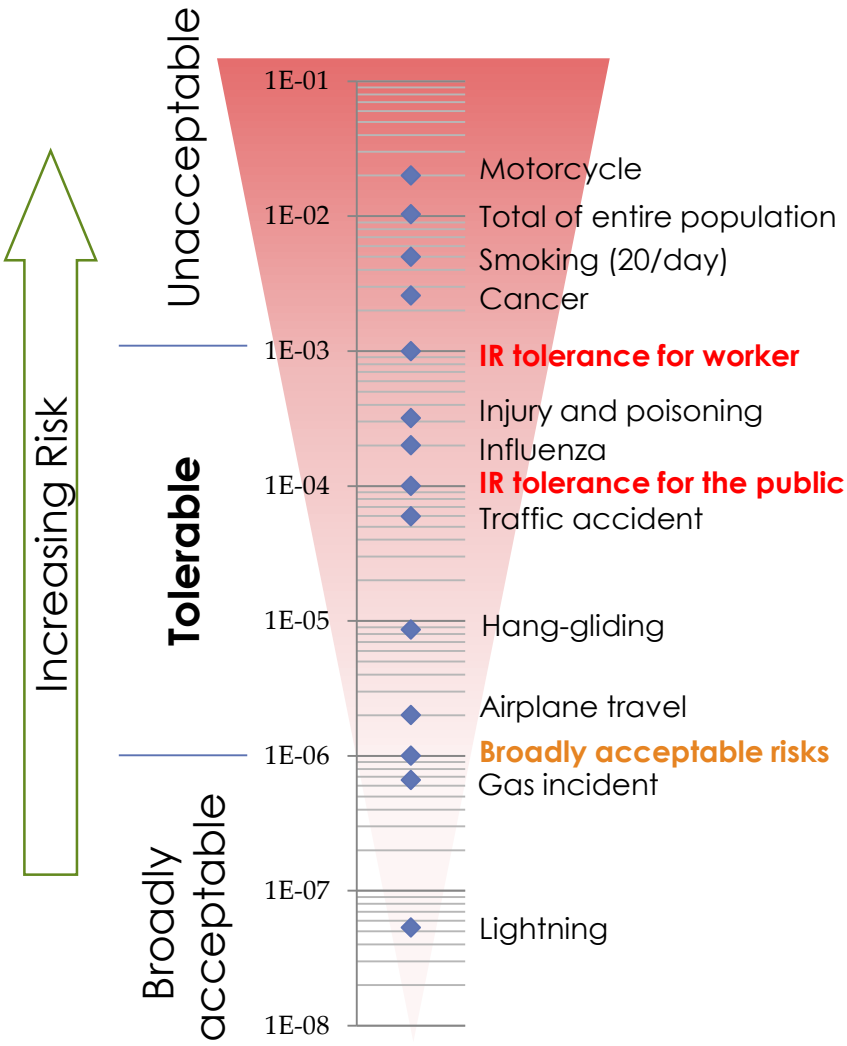

Figure 2.4 Tolerance limit of IR and the level of typical risks in life.

2.2.2 Assessment of risks

In this section, empirical equations for consequence assessment for some selected accidents are introduced.

(1) BLEVE (Boiling Liquid Expanding Vapor Explosion)

When a pressurized vessel containing a gas or liquid takes an external impact such as fire, the fluid can boil and increase the pressure of inside of the vessel. Then, a drastic explosion can occur and produce shockwave, heat from the resulted fireball, and the flying debris. This called the BLEVE, and the thermal radiation from this event can be calculated from the following equations [7], [66]–[68]. First, the maximum diameter, duration, height, and initial diameter of the fireball is calculated from the mass of leaked fluid.

$$\mathrm{D_{max}} = 5.8\mathrm{M}^{1/3} \tag{2.4}$$

$$t_{\mathrm{BLEVE}} = 0.45M^{1/3}\ for\ M < 30000kg \tag{2.5}$$

$$t_{\mathrm{BLEVE}} = 2.6M^{1/3}\ for\ M > 30000kg \tag{2.6}$$

$$H_{\mathrm{BLEVE}} = 0.75D_{\mathrm{max}} \tag{2.7}$$

$$D_{\mathrm{init}} = 1.3D_{\mathrm{max}} \tag{2.8}$$

Then, the actual distance from the center of the fireball to the receptor is obtained (Figure 2.5).

$$X_c = \sqrt{L^2 + H_{\mathrm{BLEVE}}^2} \tag{2.9}$$

$$X_s = \sqrt{L^2 + H_{\mathrm{BLEVE}}^2} - \frac{D_{\max}}{2} \tag{2.10}$$

The effect of the climate is reflected through the transmittance of the air, using the vapor pressure of water of humid air.

$$\tau_a = 2.02(P_{\mathrm{W}} X_{\mathrm{s}})^{-0.09} \tag{2.11}$$

$$P_w = 1013.25(\mathrm{RH}) \exp(14.4114 - \frac{5328}{T_a}) \tag{2.12}$$

Finally, together with the radiation coefficient (*R*, usual value is 0.3 ~ 0.4) and the heat of combustion of the fluid, thermal radiation energy is calculated as follows.

$$E_{\mathrm{r}} = \frac{2.2\tau_{\mathrm{a}} R H_{\mathrm{c}} M^{\frac{2}{3}}}{4\pi X_{\mathrm{c}}^2} \tag{2.13}$$

The probability of death can be obtained by using this probit equation.

$$Pr = -10.7 + 1.99 \ln\left(\frac{{E_r}^{1.333} t_{BLEVE}}{10000}\right) \quad (2.14)$$

(2) VCE (Vapor Cloud Explosion)

The flammable vapor cloud can be generated and accumulated if the leakage of the flammable fluid does not lead to the immediate ignition. In that case, the delayed ignition can cause explosion rather than just fire, and the shockwave from that explosion might fatality. The effect of VCE can be calculated from various methods. Here, simple TNT equivalency method is introduced [68], [69].

The mass of the flammable fluid is converted to the equivalent mass of TNT, by using the explosion efficiency (η, usual value is 0.01 ~ 0.1), the heat of combustion, and explosive energy of TNT.

$$m_{TNT} = \frac{\eta m \Delta H_c}{E_{TNT}} \quad (2.15)$$

Then, the actual distance from the explosion spot is converted to the scaled distance

$$z_e = \frac{r}{m_{TNT}^{1/3}} \quad (2.16)$$

The overpressure caused by VCE is then calculated as follows. The impulse can simply be obtained from the overpressure value.

$$p_{\mathrm{o}} = \frac{80800\left[1+\left(\frac{z_e}{4.5}\right)^2\right]}{\sqrt{1+\left(\frac{z_e}{0.048}\right)^2}\sqrt{1+\left(\frac{z_e}{0.32}\right)^2}\sqrt{1+\left(\frac{z_e}{1.35}\right)^2}} \tag{2.17}$$

$$J = \frac{1}{2} p_{\mathrm{o}} t_{\mathrm{d}} \tag{2.18}$$

The fatality due to VCE is arisen from two consequences: the impact and the lung hemorrhage. The probits can be obtained by using these equations.

$$Pr = -46.1 + 4.82 \ln(J) \tag{2.19}$$

$$Pr = -77.1 + 6.91\, ln(p_o) \tag{2.20}$$

(3) Jet fire

When the pressurized flammable gas or liquid is leaked from the vessel or pipe, the gas jet is generated due to the pressure and momentum. This can cause the directed, continuous fire. Thermal effect of this jet fire can be estimated by assuming constant flow of leaked gas, perpendicular flow direction from the leak and complete combustion. [68]

First, the radiation power is the product of the jet flow and the heat of combustion of the leaked gas.

$$Q_t = WH_c \tag{2.21}$$

The transmittance of the air is calculated from the humidity and the distance from the fire to the receptor.

$$\tau_a = 2.02(P_{\mathrm{W}}X_{\mathrm{s}})^{-0.09} \tag{2.22}$$

From the coefficient of heat capacity, temperature, molecular weight, the velocity of eruption can be obtained as follows.

$$v_s = 91.2\sqrt{\frac{\gamma T_s}{M_s}} \tag{2.23}$$

$$M_a = 0.1161\frac{W}{P_s d^2}\sqrt{\frac{\gamma T_s}{M_s}} \tag{2.24}$$

$$v = v_s M_a \tag{2.25}$$

The lower explosive limit concentration and the thrust parameter are then calculated from the jet velocity.

$$C_{LP} = C_L \frac{v}{u} \frac{M_s}{28.8} \tag{2.26}$$

$$d_j R = d \frac{v}{u} \sqrt{\frac{T_a M_s}{T_s}} \tag{2.27}$$

The thermal radiation at certain distance can be calculated using the transmittance of air, fraction of radiation (β, usual value is 0.15 ~ 0.3), total radiation power, and actual distance from the flame to the receptor. For simplicity, however, horizontal distance instead of straight-line distance can be used (Figure 2.6).

$$D = \sqrt{(L - X_c)^2 + (h + Y_c)^2} \tag{2.28}$$

$$Q = \frac{\tau \beta Q_t}{4\pi D^2} \tag{2.29}$$

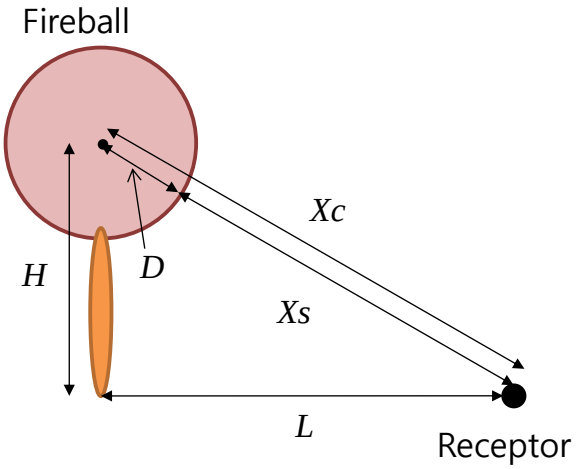

Figure 2.5 Dimensions related to consequence assessment of BLEVE (fireball).

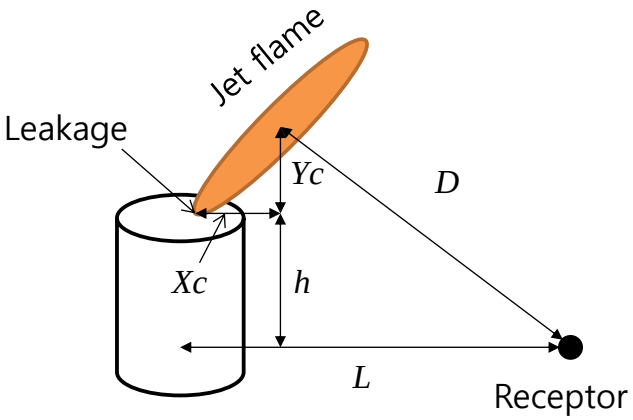

Figure 2.6 Dimensions related to consequence assessment of jet fire.

3 Risk-based Process Layout Optimization

The individual risk-based layout optimization for chemical process mainly consists of three parts. In the QRA (quantitative risk assessment) section, the hazard of the target process is analyzed. The frequency and the consequence of the identified accident scenarios are assessed to capture the risk from the process to humans. Then the risks are expressed in IR (individual risk) to be converted into the safety distances.

The layout section analyzes the process equipment and formulates the layout problem mathematically. At that time, the risk zone models developed from the safety distances are included together with the typical and additional constraints of process layout problem.

In the solution stage, iterative search procedure is used to deal with the large-scale problem which has large number of process equipment.

The overall procedure of proposed method is presented in Figure 3.1. The detailed description and the formulation of each part will follow.

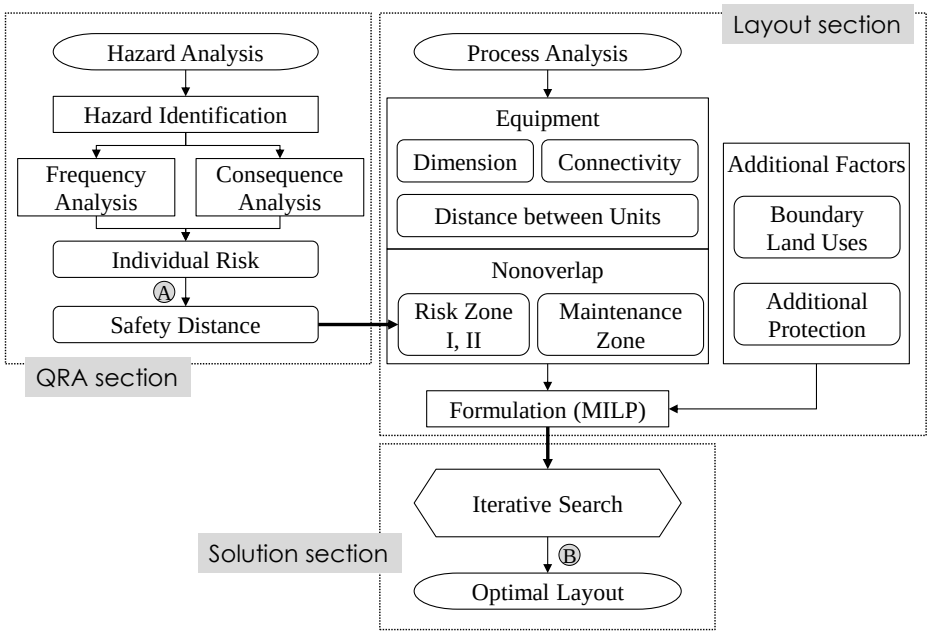

Figure 3.1 Procedure for risk-based process layout optimization.

3.1 Individual risk assessment and safety distances

The risk from process equipment can be quantified by quantitative risk assessment (QRA). Possible hazards from a target chemical process are identified and their frequency and consequences are analyzed. For frequency analysis, historical data or the frequency modeling technique can be used. For consequence analysis, there are several empirical models for each accident type such as vapor cloud explosion (VCE), fireball, flash fire or boiling liquid expanding vapor explosion (BLEVE). These models provide the quantity of thermal radiation or overpressure from an accident. Then, probit analysis [72] is applied to get the probability of fatality.

$$Pr = a + b \ln V \tag{3.1}$$

$$P = 50\left[1 + \frac{Pr - 5}{|Pr - 5|} erf\left(\frac{|Pr - 5|}{\sqrt{2}}\right)\right] \tag{3.2}$$

Generally, the product of frequency and consequence gives the measure of risk. Among several risk measures based on the QRA result, we adopted the individual risk (IR) for the risk measure to

humans in this study. IR is the risk to an individual near the hazard which considers the nature, the likelihood, and the time period of a possible injury to an individual. One of the ways to obtain IR from the frequency and consequence analysis was suggested by the Health and Safety Executive (HSE) [61]. Here, a simplified version of IR calculation assuming the worst-case accident scenario and weather- and direction-independent effects of an accident was used. In that case, IR is the product of the frequency of the event outcome *v* and the probability of fatality by the event outcome *v* at distance *r*:

$$IR_u = \sum_v f_{eo,v}\, p_{u,v}^{\mathrm{fat}} \tag{3.3}$$

HSE also proposed tolerable criteria for individual risk for people near a hazard [62]. It is recommended to keep IR lower than 10^{-3} and 10^{-4} per annum for workers who are related to the source of the hazard, and for the public, respectively.

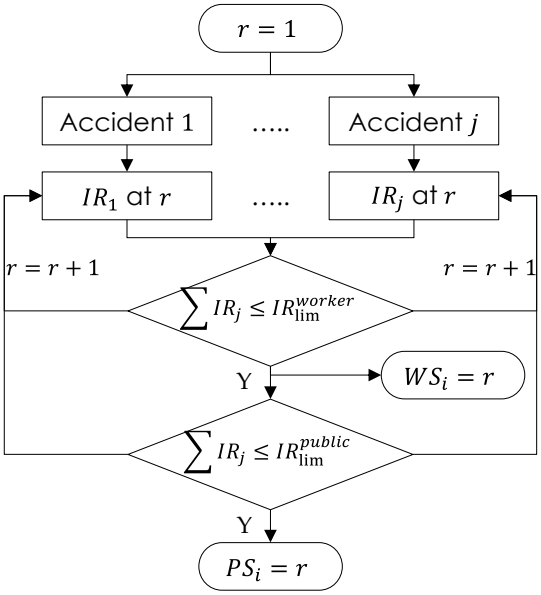

Figure 3.2 Determination of IR of equipment *i* (A in Figure 3.1).

3.2 Mathematical formulation for layout problem

The formulation in this section uses the basic MILP model from the literature [22], but most of features are modified or added to incorporate the individual risk-based safety distance constraints. For multi-floor application, additional constraints are necessary: they can be found in section 4.3.

The use of MILP formulation has practical benefits over the MINLP formulation in the process layout optimization problem. First of all, the distance between equipment, which is the major difference between the two approaches, can be expressed in more realistic measure. Since the usual pipelines connecting equipment in chemical processes meet at right angles, the rectilinear distance is a better representation of such pipeline than the Euclidean distance. In the aspect of complexity, the non-overlapping constraints of MILP formulation using the big-M method are simpler than that of the MINLP formulation using the convex hull approach. Therefore, the linear formulation for the process layout optimization is employed in this study.

3.2.1 Objective function

The major objective of the layout optimization problem is the minimization of total layout cost. In this study, the total layout cost includes cost of pipeline connection between connected equipment, purchasing required land area, purchasing of process equipment and the installation of additional protective devices.

$$\text{minimize} \sum_{i} \sum_{j \neq i} C_{ij}^{\text{pipe}} TD_{ij} + C^{\text{land}} LA + \sum_{i} C_{i}^{\text{eq}} + \sum_{i} \sum_{p} PI_{i,p} C_{p}^{\text{prot}}$$

The pipeline connection cost is the unit cost of pipeline multiplied by the rectilinear distance between connected equipment. The rectilinear distance is used to keep the linearity of the problem and reflect the actual pipeline connection in the process industry.

The cost of additional protective devices is added to the total layout cost when they are installed to the process equipment.

To keep the linearity of the problem, the land cost calculation requires some additional variables. In this study, process site can be shaped either as a square or a rectangle. For square-shaped process site, the land area is calculated from the candidates of predefined areas by using the binary variable as follows:

$$LA = \sum_{s} AR_s Q_s \tag{3.4}$$

$$AR_s = wid_s dep_s \tag{3.5}$$

$$\sum_{s} Q_s = 1 \tag{3.6}$$

$$x^{\max} = \sum_{s} wid_s Q_s \tag{3.7}$$

$$y^{\max} = \sum_{s} dep_s Q_s \tag{3.8}$$

For rectangular-shaped process site, similar calculation is used except that the selection of each side of the process site is independent by using one more binary variable.

$$LA = \sum_{s1,s2} AR_{s1,s2} Q_{s1,s2} \tag{3.9}$$

$$AR_{s1,s2} = wid_{s1} dep_{s2} \tag{3.10}$$

$$\sum_{s2} Q_{s1,s2} = Q_{s1}^{x} \tag{3.11}$$

$$\sum_{s1} Q_{s1,s2} = Q_{s2}^{y} \tag{3.12}$$

$$\sum_{s1} Q_{s1}^{x} = 1 \tag{3.13}$$

$$\sum_{s2} Q_{s2}^{y} = 1 \tag{3.14}$$

$$x^{\max} = \sum_{s1} wid_{s1} Q_{s1}^{x} \tag{3.15}$$

$$y^{\max} = \sum_{s2} dep_{s2} Q_{s2}^{y} \tag{3.16}$$

3.2.2 Risk Zone constraints

The major difficulty of layout optimization problem comes from the necessity for the prevention of overlap of equipment. This makes a disjunction:

$$[\text{Left}] \vee [\text{Right}] \vee \begin{bmatrix} \text{Above}, \text{Below} \\ [\text{Above}] \vee [\text{Below}] \end{bmatrix} \tag{3.17}$$

To model this disjunction, the big-M constraints are used for MILP formulation and the convex hull approach is used for MINLP [39]. Based on the former approach, this thesis has developed the risk zone models by modifying it and expanding it to the constraints

related to safety distances. Figure 3.3 describes the three types of risk zones and related spacing around the process equipment.

The usual representation of the effective range of the risk is a circle (or an oval). In that case, only one variable is required to model the risk zones, but the formulation of the layout problem should be MINLP, which requires more complex non-overlapping constraints. Therefore, the shapes of risk zones are set to be a square or a rectangle. In the aspect of the risk, such risk zones have the same capability to restrict the risks from the equipment since they also contain all the areas of the circular zones.

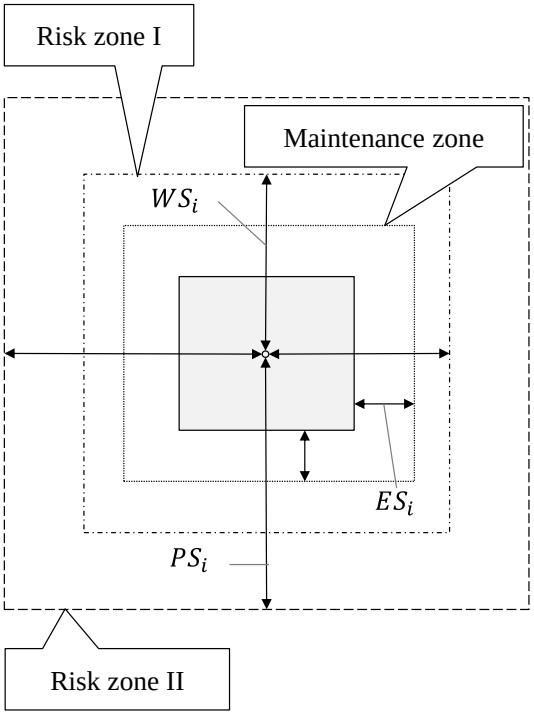

Figure 3.3 Risk zones around equipment.

(1) Maintenance zone: dimension and orientation of equipment

The maintenance zone is the sum of the area occupied by the equipment and the spacing between equipment. It is constructed simply add the spacing to the conventional 'dimension and orientation' constraints.

$$l_i = a_i O_i + b_i(1 - O_i) + 2ES_i \tag{3.18}$$

$$d_i = a_i + b_i - l_i + 4ES_i \tag{3.19}$$

Later, this maintenance zone should not be overlapped each other in any condition.

Before proceed to the next risk zone, the distance between equipment needs to be defined.

$$R_{ij} - L_{ij} = x_i - x_j \tag{3.20}$$

$$A_{ij} - B_{ij} = y_i - y_j \tag{3.21}$$

$$TD_{ij} = R_{ij} + L_{ij} + A_{ij} + B_{ij} \tag{3.22}$$

$$\forall\, i = 1, \dots, N-1,\ \ \forall\, j = i+1,\ \ \dots, N$$

When equipment *i* is on the right of *j*, the horizontal distance between the centers of them in two-dimensional plane is *R*. If *i* is on the left of *j*, it is *L*. Likewise, the vertical distances are defined as *A* or *B*. However, whether the distance is *R* (*A*) or *L* (*B*) is not explicitly determined: other binary variables are required to do that, which is not necessary for this study.

(2) Risk zone I: non-overlapping of equipment

This risk zone is for the spacing for workers based on the tolerance limit of individual risks to the workers (10^{-3} per annum). First, the basic non-overlapping constraints using big-M is as follows:

$$x_i - x_j + M\left(E1_{ij} + E2_{ij}\right) \geq \frac{l_i + l_j}{2} \tag{3.23}$$

$$x_j - x_i + M\left(1 - E1_{ij} + E2_{ij}\right) \geq \frac{l_i + l_j}{2} \tag{3.24}$$

$$y_i - y_j + M\left(1 + E1_{ij} - E2_{ij}\right) \geq \frac{d_i + d_j}{2} \tag{3.25}$$

$$y_j - y_i + M\left(2 - E1_{ij} - E2_{ij}\right) \geq \frac{d_i + d_j}{2} \tag{3.26}$$

$$\forall\, i = 1, \dots, N-1, \qquad \forall\, j = i+1, \dots, N$$

$E1$ and $E2$ are binary variables to control the application of above equations, together with appropriate large number, M. Equation (3.23) is active when $E1$ and $E2$ are both zero, otherwise, it is redundant. Likewise, Equation (3.24) is active only if $E1 = 1$ and $E2 = 0$; Equation (3.25) is active only if $E1 = 0$ and $E2 = 1$; Equation (3.26) is active only if $E1 = E2 = 1$. These constraints make the distance between two equipment greater than or equal to the sum of the half of the length of their side for both axes.

By using this concept and the restriction that the workspace should not be overlapped by a process equipment, above equations can be modified to model the Risk zone I. The distance between the workspace and equipment should be greater than or equal to the sum of the spacing for workers and the half of the length of their side:

$$x_i - x_j + M\left(E1_{ij} + E2_{ij}\right) \geq WS_i + \frac{l_j}{2} \tag{3.27}$$

$$x_j - x_i + M\left(1 - E1_{ij} + E2_{ij}\right) \geq WS_i + \frac{l_j}{2} \tag{3.28}$$

$$y_i - y_j + M\left(1 + E1_{ij} - E2_{ij}\right) \geq WS_i + \frac{d_j}{2} \tag{3.29}$$

$$y_j - y_i + M\left(2 - E1_{ij} - E2_{ij}\right) \geq WS_i + \frac{d_j}{2} \tag{3.30}$$

$$\forall\, i = 1, \dots, N - |j|, \qquad \forall\, j \in \text{workspace}$$

(3) Risk zone II: process boundary

The spacing for the public is based on the tolerance limit of individual risks to the public (10^{-4} per annum). The process equipment should be placed this amount away from the process boundary. Therefore, the restriction of the center of the equipment within the boundary can be modified to model this zone.

The basic boundary condition is as follows:

$$x_i \geq \frac{l_i}{2} \tag{3.31}$$

$$y_i \geq \frac{d_i}{2} \tag{3.32}$$

$$x_i + \frac{l_i}{2} \leq x^{\max} \tag{3.33}$$

$$y_i + \frac{d_i}{2} \leq y^{\max} \tag{3.34}$$

Then, the safety distance for the public is used instead of the equipment dimension. *PS* and *l* (*d*) are not added to avoid the duplication.

$$x_i \geq PS_i \tag{3.35}$$

$$y_i \geq PS_i \tag{3.36}$$

$$x_i + PS_i \leq x^{\max} \tag{3.37}$$

$$y_i + PS_i \leq y^{\max} \tag{3.38}$$

Although the risk from the equipment near the boundary to the public is more important than that of the equipment near the center of the site, it is not possible to determine which equipment is located near the boundary before solving the problem since the site area and the positions of equipment are both decision variables (supposition based on IR-based spacing is possible). Therefore, the Risk Zone II applies to all the process equipment regardless of their relative positions in the process site.

In addition to these boundary conditions, the factors affect the required spacing for the public based on the surrounding land uses are devised. The spacing for the public is calculated from the modified individual risk, which assumes a group of people is at the location of interest. However, the situation can vary as the land uses around the process site. For example, if a process plant borders the sea, it is not necessary to concern about the risk to that direction.

Based on this idea, four boundary factors for each direction are added to the boundary condition.

$$x_i \geq PS_i BF_{west} \tag{3.39}$$

$$y_i \geq PS_i BF_{south} \tag{3.40}$$

$$x_i + PS_i BF_{east} \leq x^{\max} \tag{3.41}$$

$$y_i + PS_i BF_{north} \leq y^{\max} \tag{3.42}$$

The value of the boundary factors can be different for the related circumstances. In this study, surrounding land uses are categorized into three types: residential, industrial and vacant areas. The residential area is the area populated with the people who are not related with the target process site, such as houses, office buildings, and public facilities. Then, *BF* for the residential area is set to 1 in order to reflect the spacing for the public as is. The industrial area refers to the other parts of the target process or the other chemical plants. The people in this area are indirectly related with the target process, so the limit of IR for them can be relaxed. Table 3.1 presents the example value of *BF*.

Table 3.1 Example of boundary factor values according to the land use types

Land use type	Boundary factor (BF)
Residential	1
Industrial	0.8
Vacant	0.5

3.2.3 Other constraints

Additional protective devices can reduce the risk from the process equipment. This causes the reduction in the required spacing for the workers and the public. The reduced spacing can be modeled by the protection factors.

$$WS_i = WS_i^{\text{init}} \left(1 - \sum_p PI_{i,p} PF_p \right) \tag{3.43}$$

$$PS_i = PS_i^{\text{init}} \left(1 - \sum_p PI_{i,p} PF_p \right) \tag{3.44}$$

PI is binary variables explaining whether or not to install the protective device *p* on process equipment *i*. Here, the superscript 'init' on *WS* and *PS* means 'initial' for the original spacing values.

3.3 Iterative search for efficient solution

As mentioned in the previous section, the binary variables (*E*1 and *E*2) in non-overlapping constraints are the major source of the complexity of the layout optimization problem. Therefore, relaxation of those constraints can help the solution to be efficient for the large-scale problem.

There is a remedy for this situation: iterative solution of the reduced problem can find the optimal point of the original problem much faster. For the layout problem, problem size can be reduced by fixing some of *E*1 and *E*2 in the proper steps among solution [28].

Figure 3.4 and the following procedure explain such method, which are adopted from the work of Xu and Papageorgiou [28] to tackle the large scale problem.

1) Initialization
   A. Initialize the iteration counter to 1.
   B. Solve the original layout problem until the first integer solution is found.
2) Release
   A. Fix all E1 and E2.
   B. Release the selected E1 and E2.
3) Solution
   A. Solve the reduced problem
   B. Compare the previous and current solutions.
4) Iteration
   A. Increase iteration counter.
   B. If the solution is not improved, and the predefined iteration limit is not reached, go to 2)

In this study, the variables to be released are selected randomly for each cycle.

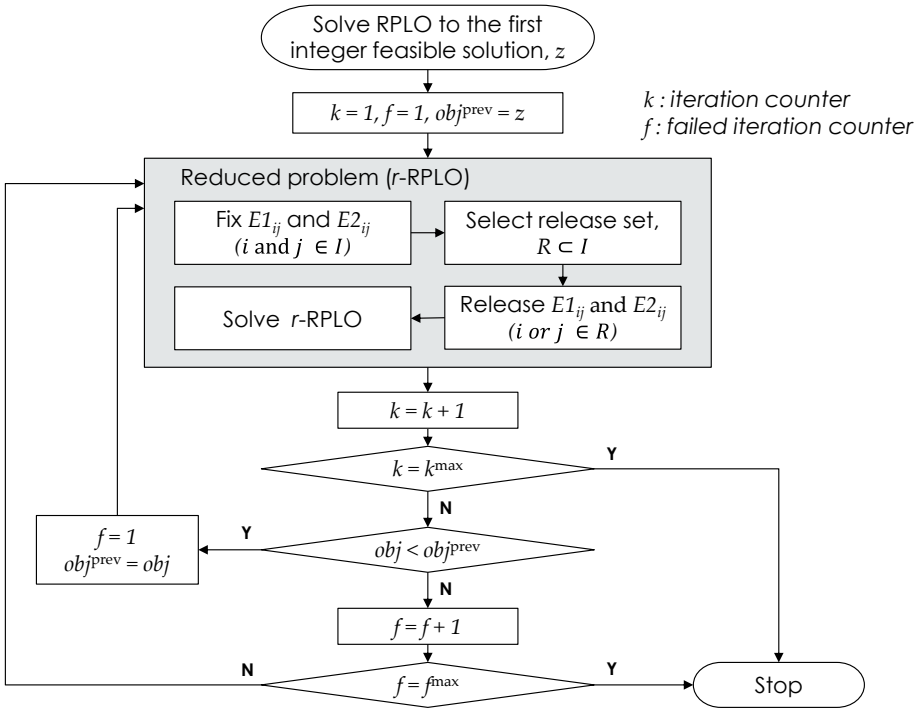

Figure 3.4 Solution of layout problem through iterative search (B in Figure 3.1).

4 Case Studies

4.1 Facility layout optimization of DME filling station†

Recently, there have been many research and discussion on the new, sustainable energy resources since the rise of energy crisis and environmental concerns on the conventional fossil fuels. Such new energy includes natural energy resources, e.g. solar, wind and tidal energy, and synthetic resources, e.g. biomass, hydrogen and gas-to-liquid (GTL) fuels [74].

Among these sustainable energy resources, synthetic fuels caught attention for their cleanness and applicability on existing industrial infra with small modification. Dimethyl ether (DME) is a promising example of it since the physical properties of DME are similar to those of diesel or liquefied petroleum gas (LPG) and the environmental impact of the combustion of DME is lower than that of the conventional fuels [75].

† This case study is an expansion of the work of Kim [73].

In Korea, several researches for DME and its commercialization as a substitute of LPG have been conducted mainly led by Korea Gas Corporation (KOGAS). Design of DME filling station in the blending process of DME, LPG and butane is an example of such research projects, and the layout optimization of facilities in that station is conducted in this study.

A DME filling station can be modeled based on the existing LPG station since they have similar physical properties and, for that reason, DME is considered as a substitute of LPG for transportation or household uses. Therefore, the layout of DME filling station should be arranged under the reflection on the same elements of that of LPG filling station.

The toxicity of DME is low [76], but it is highly flammable like LPG and other fuels, so its filling station is vulnerable to fire and/or explosion [77]. As can be seen from the incident of Bucheon, Korea in 1998 [2] and other accident cases of LPG filling stations, the safety of fuel gas filling station must be secured because they are usually allocated near the residential area. One way of securing safety is proper spacing between process equipment and populated region/building, and this study finds the optimal facility layout of DME filling station to minimize the damage to humans from the possible accident.

4.1.1 Problem statement

A DME filling station mainly consists of four units after the loading section as in Figure 4.1. DME from the source, e.g. a tank truck, is compressed and stored in a storage tank. Then, it is provided to the end users by dispensers through a pump when demanded. In addition, a building for office and/or control room is required near the process equipment [73].

Table 4.1 shows the physical dimension and the purchasing cost of equipment in the DME filling station under consideration. The storage tanks of various capacities are listed for several cases, and two dispensers are considered for layout optimization [73].

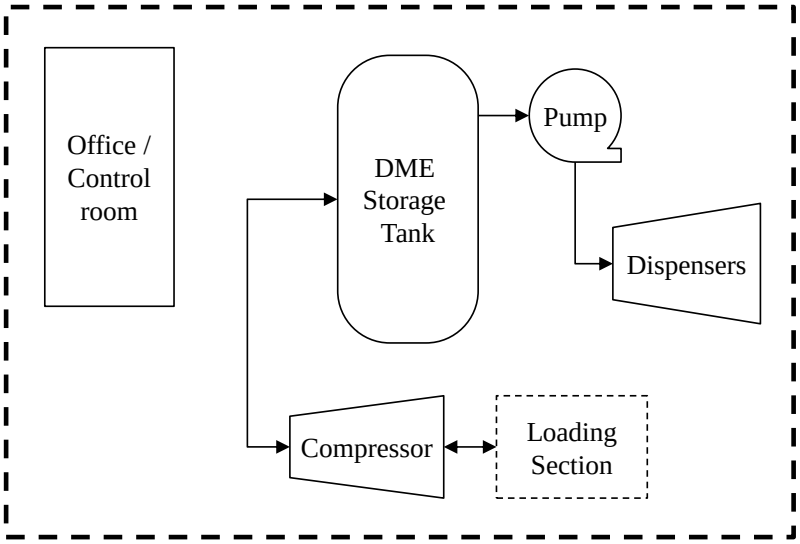

Figure 4.1 Schematic diagram of DME filling station.

Table 4.1 Equipment/facility list of DME filling station

ID	Equipment		Width [m]	Depth [m]	Capital cost [rmu*]
1	Compressor		0.8	0.6	8,700
2	Storage	5 ton	1.8	2.6	1,600
	tank	10 ton	2.5	4.1	2,100
		15 ton	2.5	6.36	2,600
		20 ton	2.5	8.76	3,100
3	Pump		0.8	0.6	700
4	Dispenser 1		0.82	0.44	1,100
5	Dispenser 2		0.82	0.44	1,100
6	Office / Control room		15	20	-

* rmu = relative monetary unit.

In this study, the following three scenarios for the allocation of the equipment/facilities in a DME filling station are examined.

(1) Simple capacity distribution

As an illustration, the layout of DME filling station with a single storage tank is optimized. Then, the storage tank is divided into various combinations of smaller tanks to find the most economical configuration. The capacity of the storage tank of the base case is 20 ton, and other combinations are followings: four 5 ton tanks, two 5 ton tanks and a 10 ton tank, a 5 ton and a 15 ton tank, and two 10 ton tanks. The purchasing costs of equipment are included in the objective function to consider the tradeoffs among the configurations of storage tanks.

(2) Effect of boundary land uses

The land uses outside the boundary of DME filling station are considered next. For this specific problem, it is assumed that residential areas are on the north and west boundaries, and the south and east boundaries are surrounded by roads which are regarded as vacant area.

Figure 4.2 depicts the surrounding land uses, and the boundary factors for that situation are shown in Table 4.2.

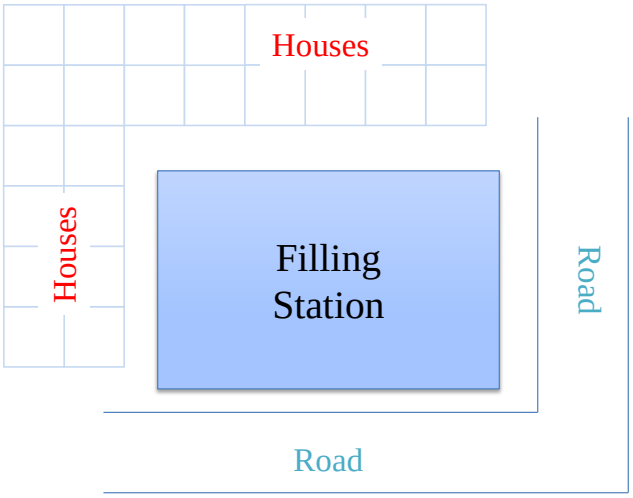

Figure 4.2 Boundary land uses around the DME filling station.

Table 4.2 Boundary factors for the DME filling station

Boundary direction	Land use type	Boundary factor, *BF*
North	Residential	1.0
West	Residential	1.0
South	Vacant	0.5
East	Vacant	0.5

(3) Installation of additional protective devices

Additional protective devices can be installed on the process equipment in order to reduce the risk further and, therefore, decrease the required safety distance. Since their installations do cost, an optimal point can be found between full protection and large process area.

The cost and the risk reduction factors of additional protective devices available for DME filling station are shown in Table 4.3 [78]. The cost of protective device is included in the objective function. It is assumed that the effect of each protective device on IR is independent so that the total risk reduction factor is the sum of each reduction factor which is installed to that equipment.

Table 4.3 Available protective devices for additional installation

ID	Protective devices	Installation cost [rmu]	Risk reduction factors
1	Additional cooling water	500	0.1
2	Additional overpressure relief devices	2000	0.24
3	Additional fire relief devices	2500	0.25

4.1.2 Risk calculation

The risk indices for DME filling station is evaluated by analyzing the historical accident database of LPG filling stations which is a similar process to this case. Accident records from 1987 to 2003 in Korea are investigated [79], and three major types of accident are identified: flash fire, BLEVE (boiling liquid expanding vapor explosion), and VCE (vapor cloud explosion). Flash fire and VCE are modeled for all four major pieces of equipment in the DME filling station while BLEVE is modeled only for the storage tank. With these types of accident scenarios and operation conditions of equipment, a probit model for accident effect evaluation is built to be used for individual risk calculation.

Figure 4.3 shows how the equipment's risk boundary was determined from the IR value. The dashed line represents the IR limit for workers (10^{-3} per annum) and for the public (10^{-4} per annum). Since the fatality rate terms of IR calculation varies with the distance from the equipment, the minimum distance that meets the IR tolerance limit can be obtained by using this chart. For example, the dispenser should be placed 25 m or more away from workspace because that is the minimum distance below the IR limit for workers (only the integer numbers for distance are taken).

The risk boundary distances and the IR values at those distances are listed in Table 4.4 for the equipment in the DME filling station. Since there is no prescribed regulation for the spacing between equipment in DME filling station, general recommended spacing for storage tank, pump, and compressor are brought from the literature [80]. For the dispensers, we assumed it to have the spacing value between that of the storage tank and the pump.

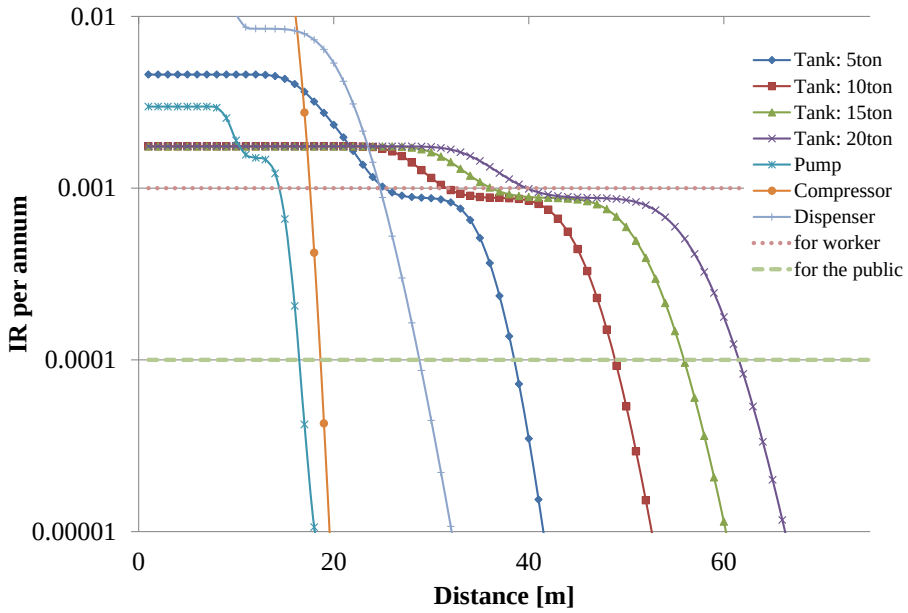

Figure 4.3 IR of equipment in the DME filling station.

Table 4.4 Required spacing based on the IR of equipment

Equipment		For worker		For the public		Between equipment
		WS [m]	*IR* [10^{-3}yr^{-1}]	*PS* [m]	*IR* [10^{-4}yr^{-1}]	*ES* [m]
Storage tank	5ton	26	0.94	39	0.72	7.7
	10ton	31	0.97	49	0.93	
	15ton	37	0.96	56	0.96	
	20ton	40	0.99	62	0.83	
Pump		15	0.66	17	0.42	8.8
Compressor		18	0.42	19	0.42	9.6
Dispenser		25	0.88	29	0.86	8

4.1.3 Layout result and discussion

The optimization problem is formulated as MILP and solved in GAMS [81] with ILOG CPLEX solver to minimize the total cost of layout of DME filling station.

In addition to the constraints of the formulation in the chapter 3, some constraints were added for the dispensers to reflect the characteristics of real-world filling station. First, the following three equations restrict the two dispensers to be located next to each other and near the boundary.

$$R_{i,j} - L_{i,j} = 0 \tag{4.1}$$

$$A_{i,j} - B_{i,j} = \frac{d_i + d_j}{2} \tag{4.2}$$

$$x^{\max} - x_i \leq PS_i \tag{4.3}$$

$$i, j \in \{4,5\}$$

These additional constraints can also remove degeneracy in the layout results.

If some additional protective devices are applied to a dispenser, they are also applied to the other dispenser. This situation is controlled by the following constraint.

$$PI_{i,p} = PI_{j,p} \tag{4.4}$$

$$i, j \in \{4,5\}$$

(1) Simple capacity distribution

As the first case, simply the layout of the facilities of the DME filling station with a single 20 ton storage tank is optimized in square-shaped process site.

The resulted layout is depicted in Figure 4.4. The storage tank is allocated near the center of the process site, the farthest point from the public area (process boundary) because they cause the highest individual risk. On the other hand, the control room/office building, which is assumed as the space for workers, is placed on the corner of the site because they do no harm to the public but only take the risk from other equipment. Figure 4.5 shows the risk contours of process equipment for the base case. The dashed and solid circles represent the risk contours for workers and the public, respectively. It can be easily checked that the risk contours for the public (IR < 10^{-4}) do not cross the process boundary.

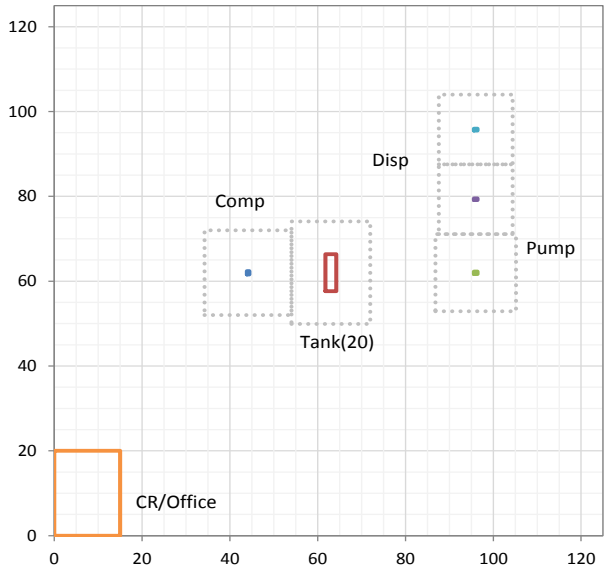

Figure 4.4 Optimal layout of DME filling station – Base case: 20 ton.

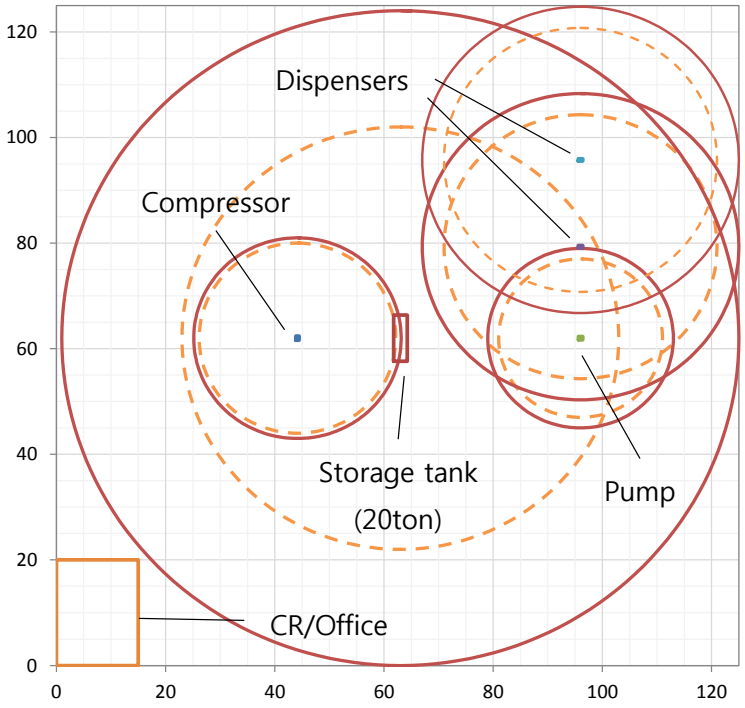

Figure 4.5 Risk contours for Base case.

Next, the storage tank is divided into smaller ones. The layout results for the Case 1 through Case 4 are shown in Figure 4.6 – Figure 4.9. The storage tanks are also located near the center of the process site, and the CR/office is on the corner.

As can be seen in the figures, the resulted land areas are different for each case. Smaller tanks have lower risk than larger ones because they contain smaller amount of hazardous material, in this case, DME, so they require less space to meet the IR tolerance. However, cost of purchasing storage tank is not proportional to its capacity. This make the tradeoff between land cost and purchasing cost, and therefore, an optimal configuration can be found. In this case study, the combination of a 15 ton and a 5 ton storage tank (Case 3) was the optimal layout. The detailed cost and layout results are summarized in Table 4.5 and Figure 4.10.

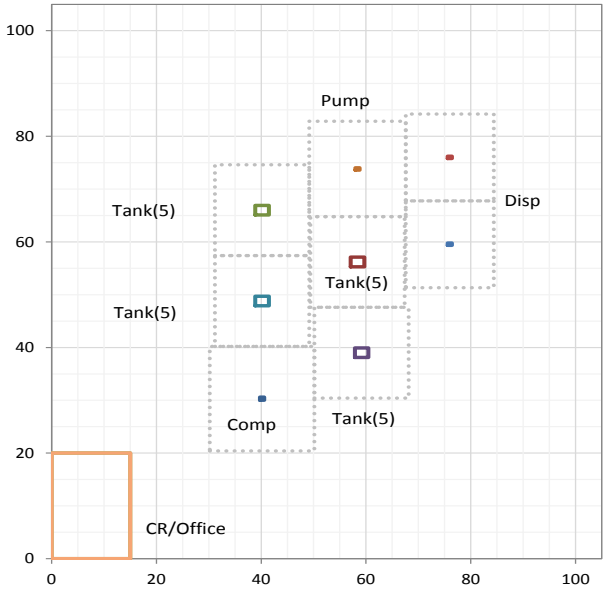

Figure 4.6 Optimal layout of DME filling station – Case1: 5ton x 4.

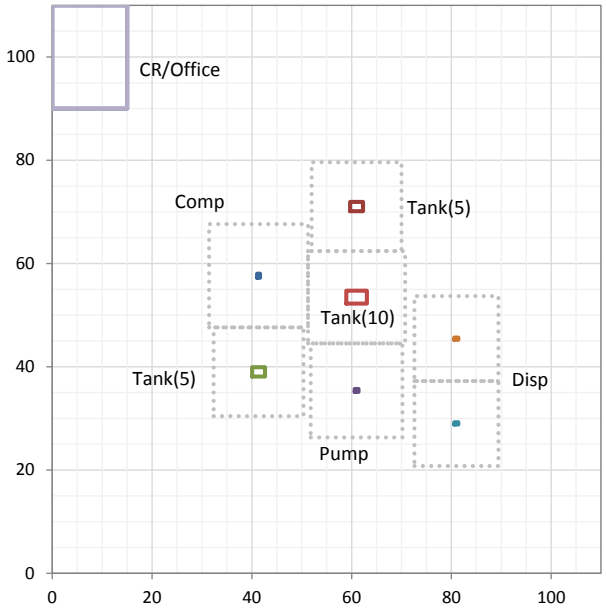

Figure 4.7 Optimal layout of DME filling station – Case2: 5 ton x 2 + 10 ton.

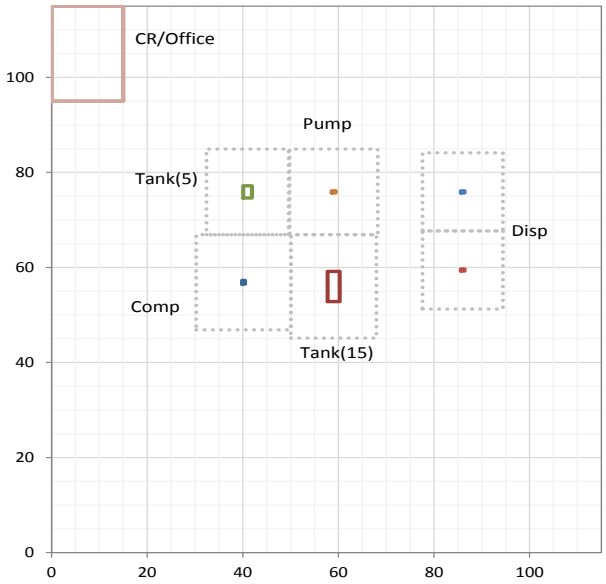

Figure 4.8 Optimal layout of DME filling station

– Case3: 5 ton + 15 ton.

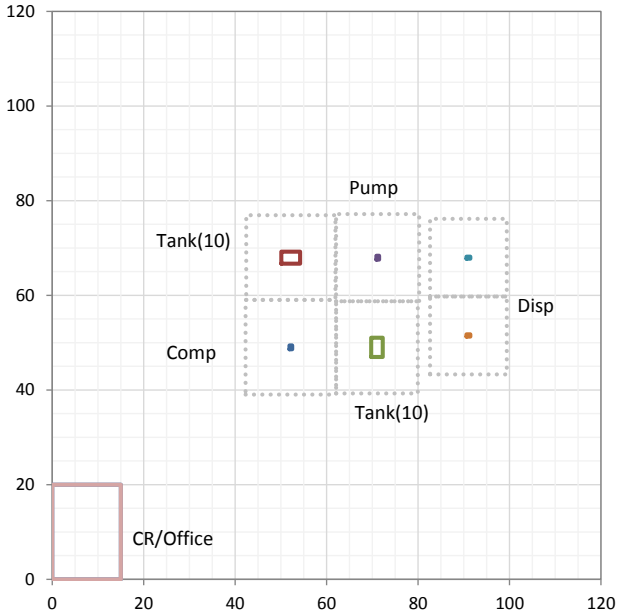

Figure 4.9 Optimal layout of DME filling station – Case4: 10 ton x 2.

Table 4.5 Cost comparison of capacity distribution cases

Cases		Cost				Site		
		Connection [rmu]	Land [rmu]	Equipment [rmu]	Total [rmu]	x^{max} [m]	y^{max} [m]	LA [m^2]
Case1	5x4	40824	72765	18000	131589	105	105	11025
Case2	5x2 +10	28395	79860	16900	125155	110	110	12100
Case3	15 + 5	21598	87285	15800	124683	115	115	13225
Case4	10x2	15257	95040	15800	126098	120	120	14400
Base	20	13998	103125	14700	131823	125	125	15625

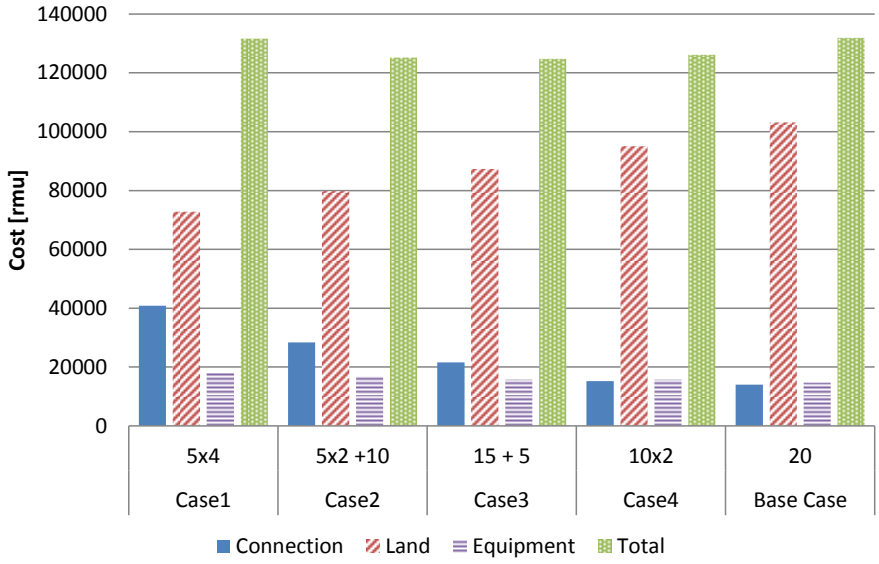

Figure 4.10 Cost comparison of capacity distribution cases.

Simple sensitivity analysis for the effect of some parameters on total layout cost has been conducted for the optimal case (Case 3). The unit cost of pipeline connection and land, and equipment price were varied, and their impacts on total cost are illustrated in Figure 4.11. The land cost shows the strongest correlation, while the other two parameters have negligible effect. The land cost has great impact on the fuel gas station in urban area in real world, so the result of sensitivity analysis can be regarded as acceptable.

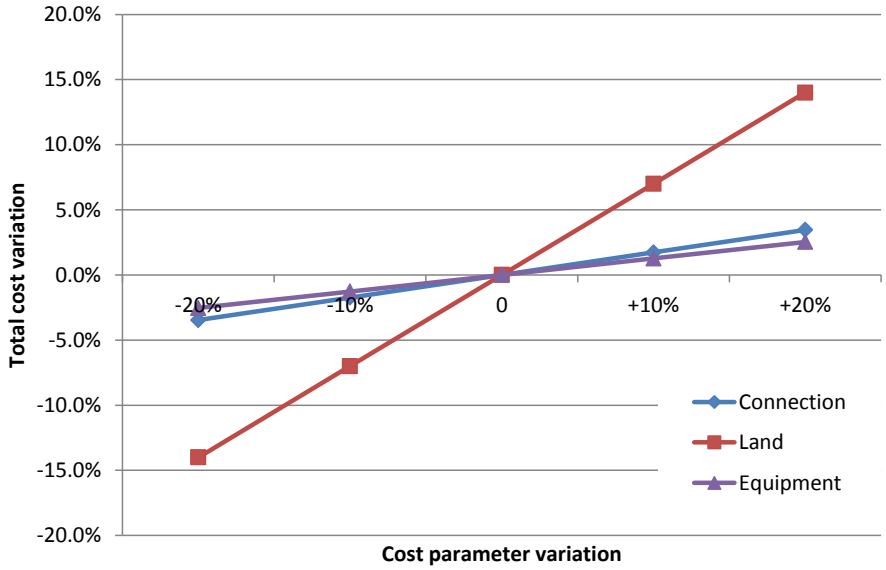

Figure 4.11 Effect of parametric variations for Case 3.

(2) Effect of boundary land uses

Since the fuel gas station is usually built in urban area, it is important to consider the surrounding land uses in layout optimization. Four directions outside the boundary of DME filling station are assumed to be residential areas and roads.

Figure 4.12 shows the resulted layout. The process equipment tends to be allocated near the boundaries with vacant land uses, since the effective range of individual risk for the vacant land uses is smaller than that for the residential land uses. The land area is shrunk in comparison with Figure 4.4 because the boundary factors other than the residential area decrease the required spacing.

For this scenario, the result using the formulation for rectangular site was the same as the square case. Detailed layout result is shown in Table 4.6.

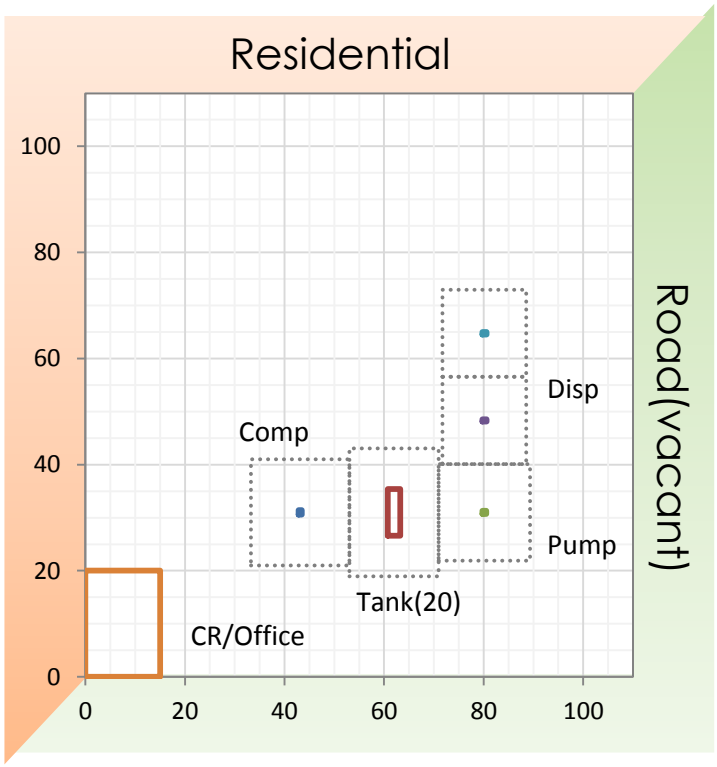

Figure 4.12 Optimal layout of DME filling station with boundary factors.

(3) Installation of additional protective devices

The layout results considering the effect of additional protective devices are shown in Figure 4.13, Figure 4.14 and Table 4.6. The addition of protection dramatically reduces the risk from the equipment, and therefore, the resulted process sites are much smaller than the previous cases.

One might expect the additional protective devices on the storage tank can be beneficial since it has the greatest risk among the equipment in DME filling station. Actually, all three protective devices were set to be installed on the storage tank for both cases of square and rectangle. For the other equipment, various configurations from zero to two installations were applied.

Among all the cases of the DME filling station with 20 ton capacity, the rectangular site with the consideration of the boundary factors and protection factors result the lowest total cost of layout. Parametric sensitivities on the total cost are analyzed for this case and illustrated in Figure 4.15. Like the preceding, the land cost (LC) has great influence. Spacing for the public (PS) has also large impact because it affects the land area, while the effect of WS (spacing for workers) is diminished by PS. Protection factor by additional protective devices (PF) shows negative effect on total cost, naturally.

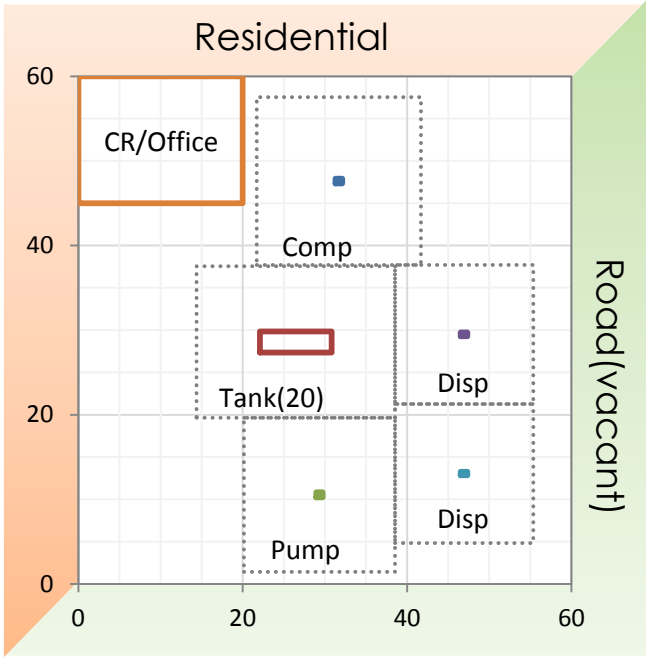

Figure 4.13 Optimal layout of DME filling station with additional protective devices installed (square site area).

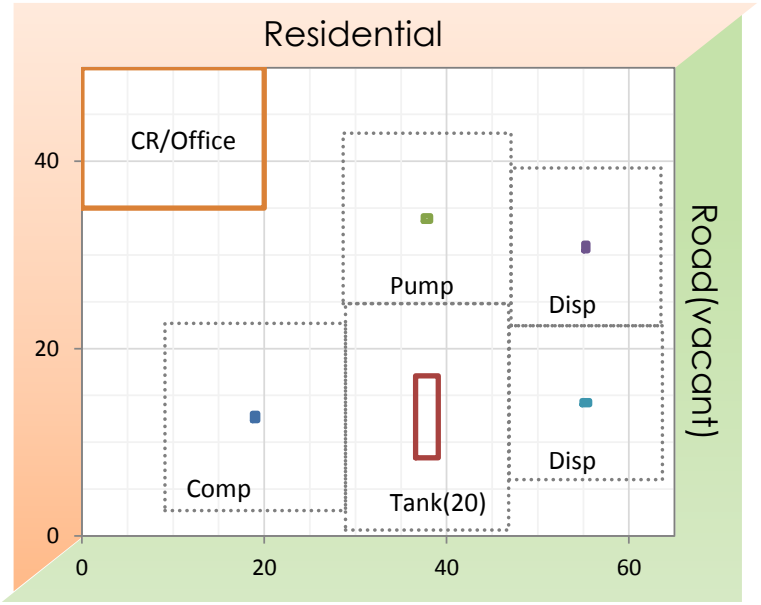

Figure 4.14 Optimal layout of DME filling station with additional protective devices installed (rectangular site area).

Table 4.6 Result summary for DME filling station

BF	PF	Shape*	Cost					Site		
			Connection [rmu]	Land [rmu]	Equipment [rmu]	Protection [rmu]	Total [rmu]	x^{max} [m]	y^{max} [m]	LA [m^2]
X	X	S	21598	87285	15800	-	124683	115	115	13225
		S	11978	59565	-	-	71543	95	95	9025
O	X									
		R**	11978	59565	-	-	71543	95	95	9025
		S	13850	23760	-	9000	46610	60	60	3600
O	O									
		R	13268	21450	-	10500	45218	65	50	3250

* S = Square, R = Rectangle.

** Resulted site was a square.

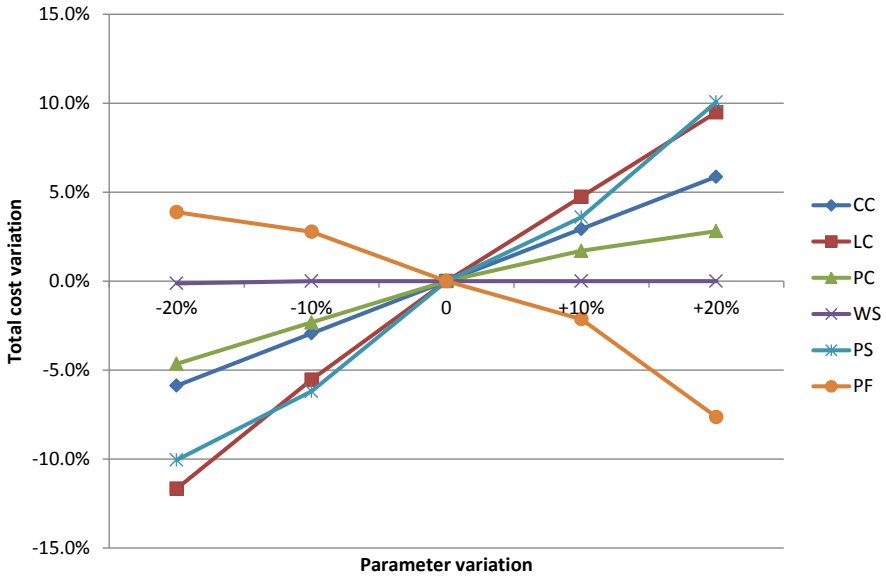

Figure 4.15 Effect of parametric variation for optimal case.

For this case study, the benefit of the proposed method is the reduced land area for the layout, and therefore, the reduced cost. As can be seen from Table 4.7, proposed method reduced 20% of the land area required for a DME filling station with a single 20 ton storage tank than the previous result. This is because the risk zones modeling and non-overlapping constraints for them in the proposed formulation. They made the relative allocation of process equipment more efficient, and removed the unnecessary spacing between equipment.

Moreover, only 17% of land area is required when the boundary land use and additional protective devices were considered. This can support the decision making related with the siting and additional safety measures.

Table 4.7 Result comparison for single 20 ton case

	Kim (2011)	Proposed	Proposed (with BF and PF)
Land area [m^2]	19,600	15,625	3,250
Relative value [%]	100	80	17

4.2 Optimal layout of ethylene oxide plant

Ethylene oxide (EO) is one of the most important raw materials used in the chemical industries. The synthesis of ethylene glycols such as diethylene glycol and triethylene glycol is the major application of EO. Ethylene glycol ethers, ethanolamines and ethoxylates are also important products from EO [82].

EO is synthesized by direct oxidation of ethylene by air or purified oxygen. A fresh ethylene is oxidized into ethylene oxide in a catalytic plug flow reactor. The hot product gases are cooled and EO is stripped out by water-based absorber. Remaining gases are further cooled and the byproduct (carbon dioxide) is removed in the second absorber. The rest of this process is for the recycle [31].

Although EO is an essential material, it is also a hazardous chemical with high reactivity and toxicity. National Fire Protection Agency (NFPA) designated EO as Class 1A flammable liquid [83], and Environmental Protection Agency (EPA) regulates it as an extremely hazardous substance [84]. Therefore, the production and handling of EO need specific cares.

The risk assessment study of EO plant [85], [86] says that both ethylene and EO is vulnerable to fire and explosion and the most part

of the plant is regarded as hazardous (H) or highly hazardous (HH) in SWeHI (Safety Weighted Hazard Index).

Several researches have been conducted for the layout of the EO plant. An MINLP approach for safe process plant layout regarding the financial risk of possible accident [31], MILP approach for single floor [26] and multi floor [23] layout optimization without the safety consideration are some example of them. These approaches usually tried to prevent the accident among the process equipment only. However, the accident in EO plant can affect not only the process equipment, but also, and more importantly, the people nearby. This is why direct consideration of the risk to humans is required in the arrangement of layout of EO plant.

4.2.1 Problem statement

An EO plant mainly consists of seven units: a reactor, two heat exchangers, two absorbers, a flash drum and a pump [31]. The connectivity among the equipment is shown in the simplified diagram of major units of EO plant in Figure 4.16. Physical dimensions, prices and the connectivity information are listed in Table 4.8 [22].

Three types of workspaces for employees are added to the layout – a laboratory, a control room and an office building. Their

relative locations are restricted to be next each other, in order to prevent the degeneracy of the solution and to reflect the reality.

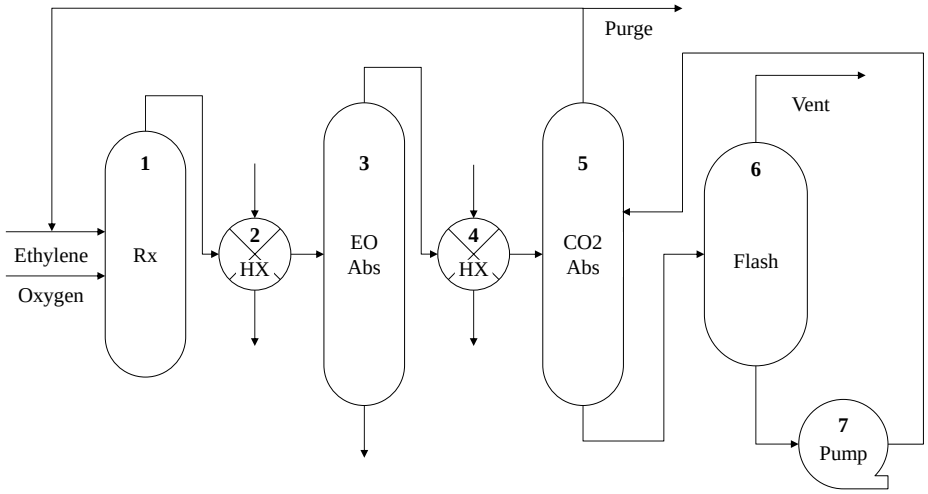

Figure 4.16 Process flowsheet of EO plant.

Table 4.8 Equipment information of EO plant

Equipment		Width [m]	Depth [m]	Purchasing cost [$]	Connectivity	Connection cost [$/m]
1	Rx	5.22	5.22	335000	(1,2)	346
2	HX1	11.42	11.42	11000	(2,3)	118
3	EO Abs	7.68	7.68	107000	(3,4)	111
4	HX2	8.48	8.48	4000	(4,5)	85.3
5	CO2 Abs	7.68	7.68	81300	(5,1)	416.3
6	Flash	2.6	2.6	5000	(5,6)	86.3
7	Pump	2.4	2.4	1500	(6,7)	6.5
					(7,5)	82.8

First, simple layout optimization of EO plant is conducted as an illustration. The shape of the process site is assumed to be both square and rectangle.

Secondly, a hypothetical decision making problem is considered. A new EO plant is going to be constructed but there are two options for location of process site. Site 1 and Site 2 are both surrounded by the sea on one side, other chemical plants on two sides, and residential/business zone on one side as depicted in Figure 4.17. The choice between the two alternatives might be tricky since they have the same combinations of boundary land uses, but their directions are different. The candidate that can achieve the lowest layout cost while satisfying the IR tolerance would be selected. The boundary factors for each option are listed in Table 4.9.

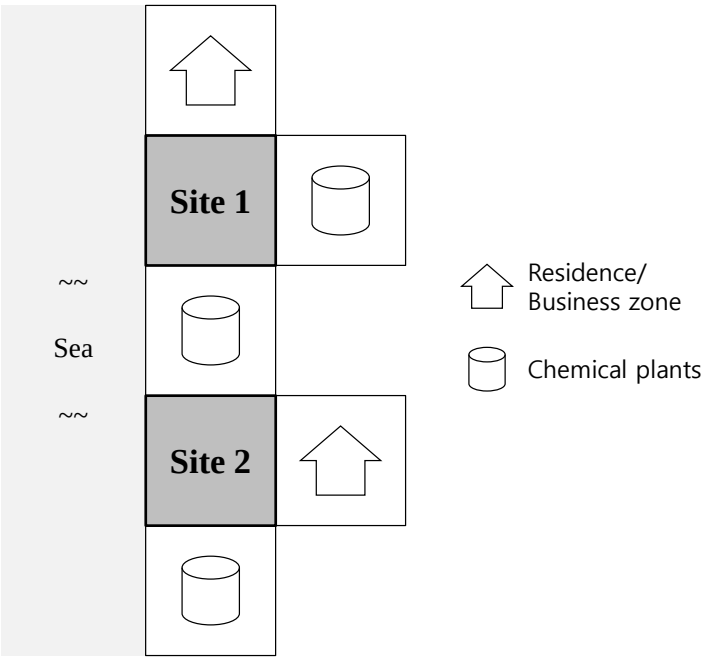

Figure 4.17 Land uses around the candidate EO plant sites.

Table 4.9 Boundary factors of site options

Boundary	Site option 1		Site option 2	
	Land use	BF	Land use	BF
West	Vacant	0.5	Vacant	0.5
South	Industrial	0.8	Industrial	0.8
East	Industrial	0.8	Residential	1.0
North	Residential	1.0	Industrial	0.8

After the second problem, site selection is reconsidered with the additional protections. There are seven protective devices available, and information on additional installation of protective devices is presented in Table 4.10 [26].

The protective devices reduce the risk from the process equipment and therefore, the required land area; however, additional costs are also required to achieve it. This leads to a decision making problem for selection of additional protective devices.

Unlike the case of the DME filling station, the additional protection can be installed only on the reactor and absorbers. Moreover, the applicable configurations of protective devices are set beforehand as in Table 4.11 [26].

Table 4.10 Additional protective devices available for EO plant

	Protective Device	Installation cost [$]	Risk reduction factor
P1	Additional cooling water	5000	0.1
P2	Additional overpressure relief devices	20000	0.24
P3	Additional fire relief devices	15000	0.25
P4	Second skin on reactor	65000	0.6
P5	Explosion protection system on reactor	20000	0.2
P6	Duplicate control system with interlocking flow on reactor	20000	0.32
P7	Duplicate control shutdown system on absorption tower	30000	0.46

Table 4.11 Applicable configurations of the protective devices

Configuration	Reactor	Absorbers
K1	-	-
K2	P1	P1
K3	P3	P2
K4	P1,P3,P6	P1,P2
K5	P1,P3,P5,P6	P1,P7
K6	P1,P3,P4,P5,P6	P1,P2,P7

4.2.2 Risk calculation

The modified individual risks from the process equipment of the EO plant are calculated from the frequency and the consequence analysis results of the possible hazards.

For the equipment in EO plant, the accident types including vapor cloud explosion (VCE), flash fire, jet fire and fireball are considered. Using the failure rate data and event tree analysis (ETA), the frequencies of each accident scenario for all the equipment were obtained. Then, consequences, i.e. the overpressure from VCE and thermal radiation from the three types of fires were calculated by using the known empirical equations.

The resulting individual risks depending on the distances from the centers of the process equipment are presented in Figure 4.18. The minimum distances those satisfy the tolerance limits of IR are determined as the required spacing for workers (10^{-3} per annum) and for the public (10^{-4} per annum). Such spacing values and the IR at those distances are listed in Table 4.12, together with the minimum clearance distances between equipment which brought from the literature [87]. The minimum clearance is necessary for the maintenance purpose, and somewhat reduces the probability of domino effect.

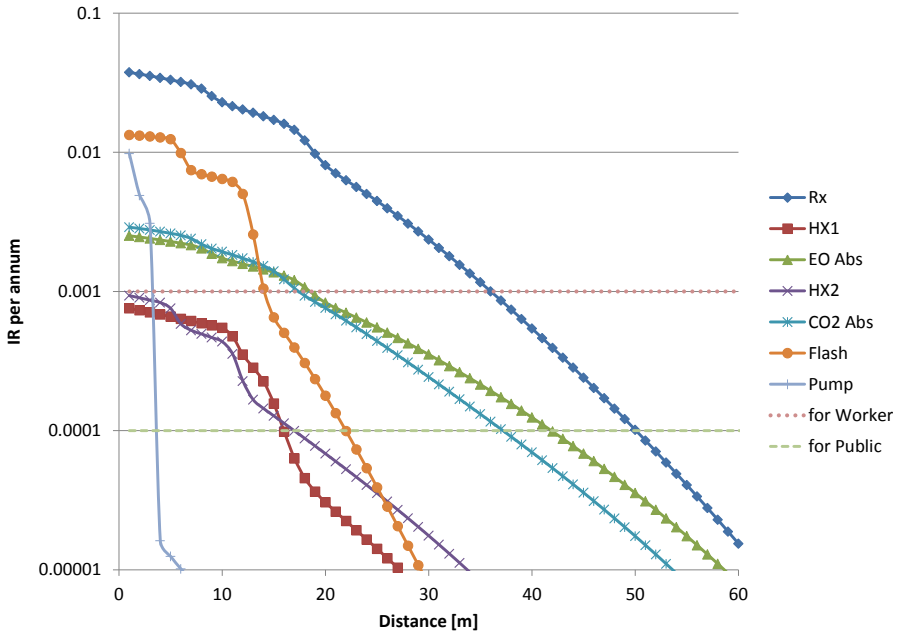

Figure 4.18 IR of major equipment in the EO plant.

Table 4.12 Required spacing based on IR of equipment in EO plant

Equipment	For worker		For the public		Minimum clearance
	WS [m]	*IR* [10^{-3}yr^{-1}]	*PS* [m]	*IR* [10^{-4}yr^{-1}]	*ES* [m]
Rx	37	0.862	51	0.847	4.2
HX1	1	0.756	16	0.981	2.3
EO Abs	19	0.933	42	0.985	3.2
HX2	1	0.934	17	0.996	2.3
CO2 Abs	18	0.931	38	0.902	3.2
Flash	15	0.65	22	0.991	3.2
Pump	4	0.0162	4	0.162	1

4.2.3 Layout result and discussion

(1) Simple layout

The layout results of the EO plant based on IR consideration are presented in Figure 4.19, Figure 4.20 and Table 4.13. The rectangular site cost less that the square case, but there is only a little difference between them. The reactors are placed near the center of the process site for both cases, since they can cause greater risk than the other equipment.

When compared to the layout results from the former literatures, it can be noticed that the relative positions of process equipment are almost the same with the other research except the spaces between equipment due to the minimum clearance constraints. This can be interpreted that the safety distances for the workers and the public do not have impact on the relative arrangement inside the process boundary. However, this situation becomes different when the boundary factors are considered next.

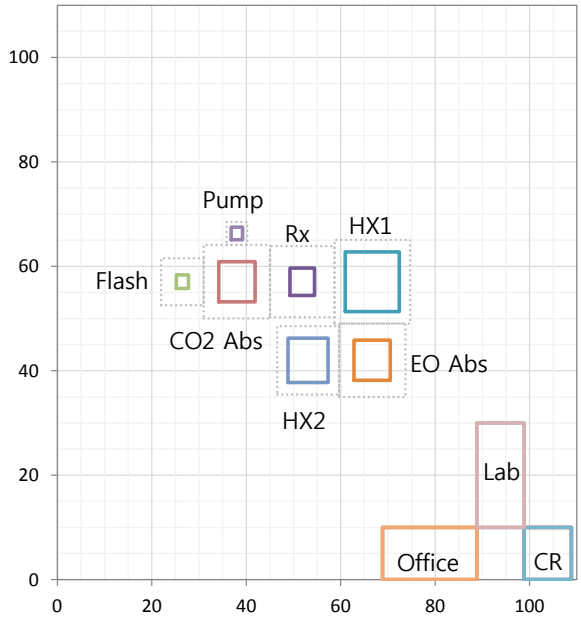

Figure 4.19 Optimal layout of EO plant – Square site.

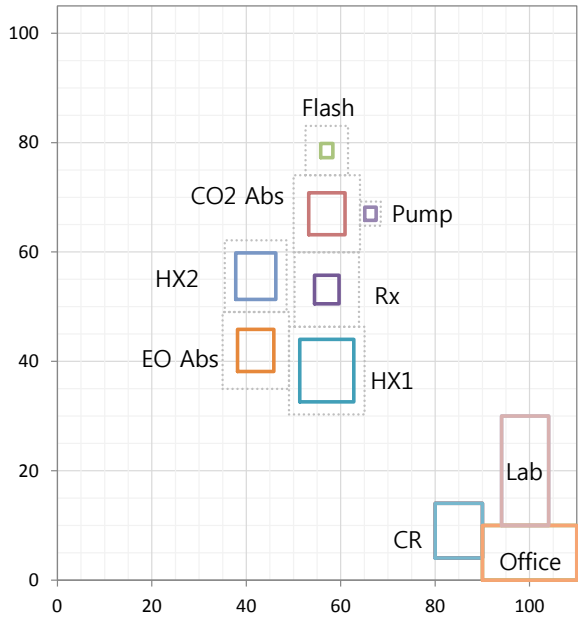

Figure 4.20 Optimal layout of EO plant – Rectangular site.

Table 4.13 Layout result of base case for EO plant

		Square	Rectangle
Cost	Connection [$]	18643.74	18763.75
	Land [$]	321860	307230
	Total [$]	340503.7	325993.8
Site	x^{max} [m]	110	110
	y^{max} [m]	110	105
	LA [m^2]	12100	11550

(2) Site selection

The most economical layout between the two candidate sites is determined. Figure 4.21 presents the case of Site 1 where the residential/business zone is on the north of the process site, while Figure 4.22 shows the case of Site 2 where that region is on the east. The detailed comparison for the site options are on Figure 4.23 Table 4.14. The rectangular layout on Site 1 was the optimal layout among four cases, but there were not much gap for total costs except the square layout on Site 1.

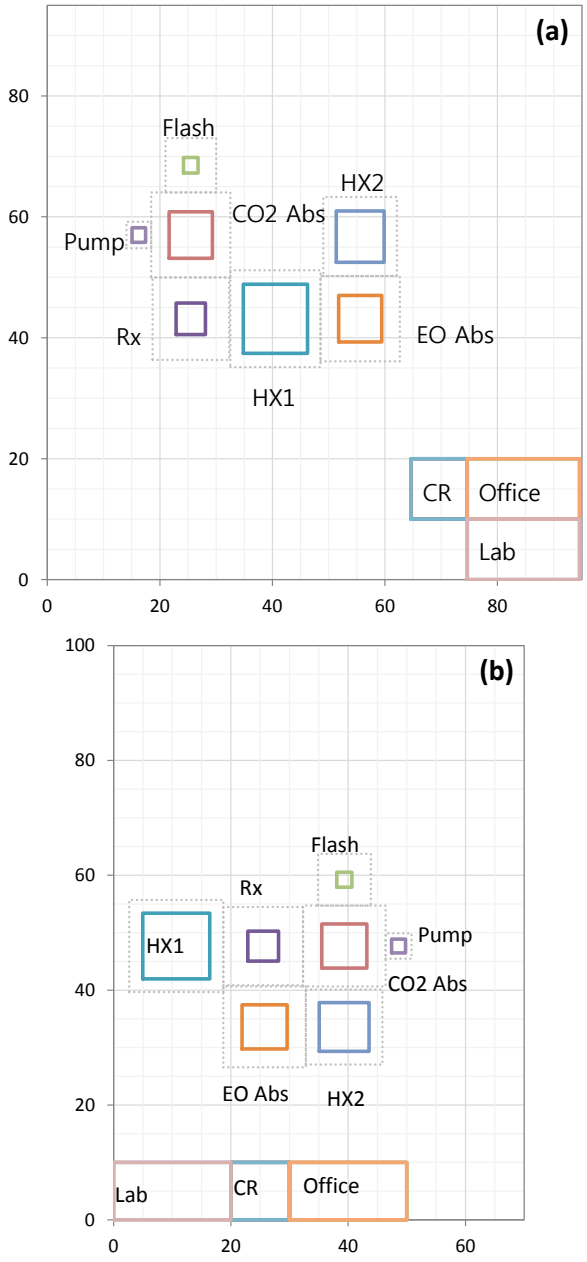

Figure 4.21 Optimal layout of EO plant in site option 1 (a) square site (b) rectangular site.

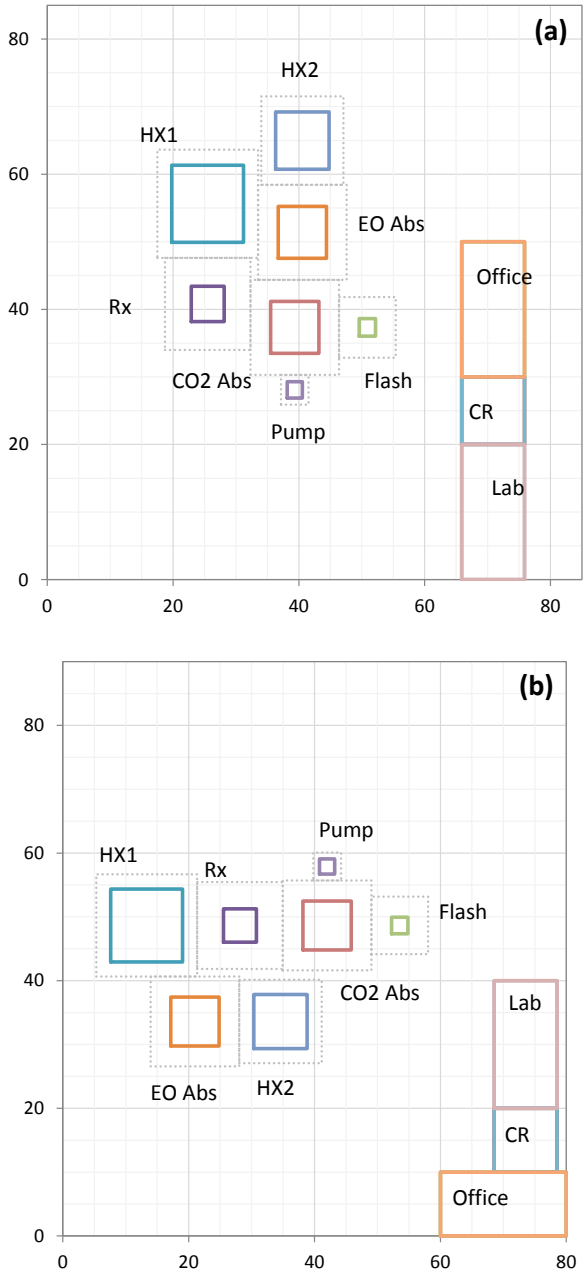

Figure 4.22 Optimal layout of EO plant in site option 2 (a) square site (b) rectangular site.

Table 4.14 Layout result of EO plant with boundary factors

		Option1		Option2	
Cost	Connection [$]	18742.94	18938.68	20481.24	18894.55
	Land [$]	240065	186200	192185	191520
	Total [$]	258807.9	205138.7	212666.2	210414.6
Site	Shape	Square	Rectangle	Square	Rectangle
	Width [m]	95	70	85	80
	Depth [m]	95	100	85	90
	Area [m^2]	9025	7000	7225	7200

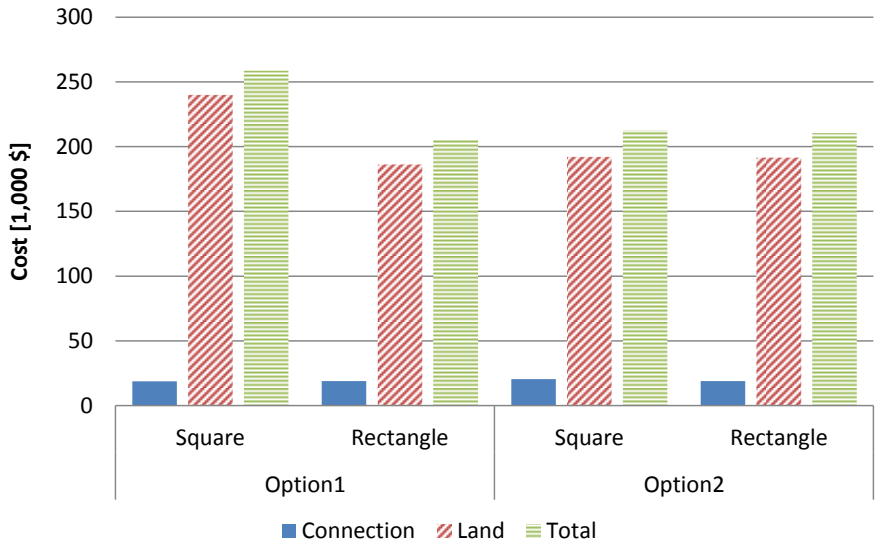

Figure 4.23 Cost comparison of the site selection problem for the EO plant.

(3) Site selection with additional protective devices

The last case is the site selection revisited. The boundary factors were kept but the effect of additional protection is considered. The cost, site dimension and the installed protective devices are summarized in Table 4.15, and the plane views of the resulting layouts are depicted in Figure 4.24 and Figure 4.25.

For Site 1, the workspaces are placed near the north boundary, where the residential/business zone is located. This happens on the east boundary for Site 2. This is because the workspaces are assumed to do no harm to the public. Moreover, by moving them to the residential boundary, the required land area can be reduced.

The most selected configuration of protective device was K2, which installs P1. Actually, this result can be anticipated from the information of the protective devices: the cost required to reduce the same amount of risk is the lowest for P1. That is, P1 cost $5,000 for 10% risk reduction, while P3 cost $10,833 for the same protection.

It can be noticed that the parameters affect the land size (BF, PS, PF) and the land cost have the greatest effect on the total layout cost as in Figure 4.26.

Finally, Figure 4.27 illustrates the risk zones in the optimal layout case (Site 1, rectangle). All the risk zones are confined within the process area and do not overlap with the workspaces.

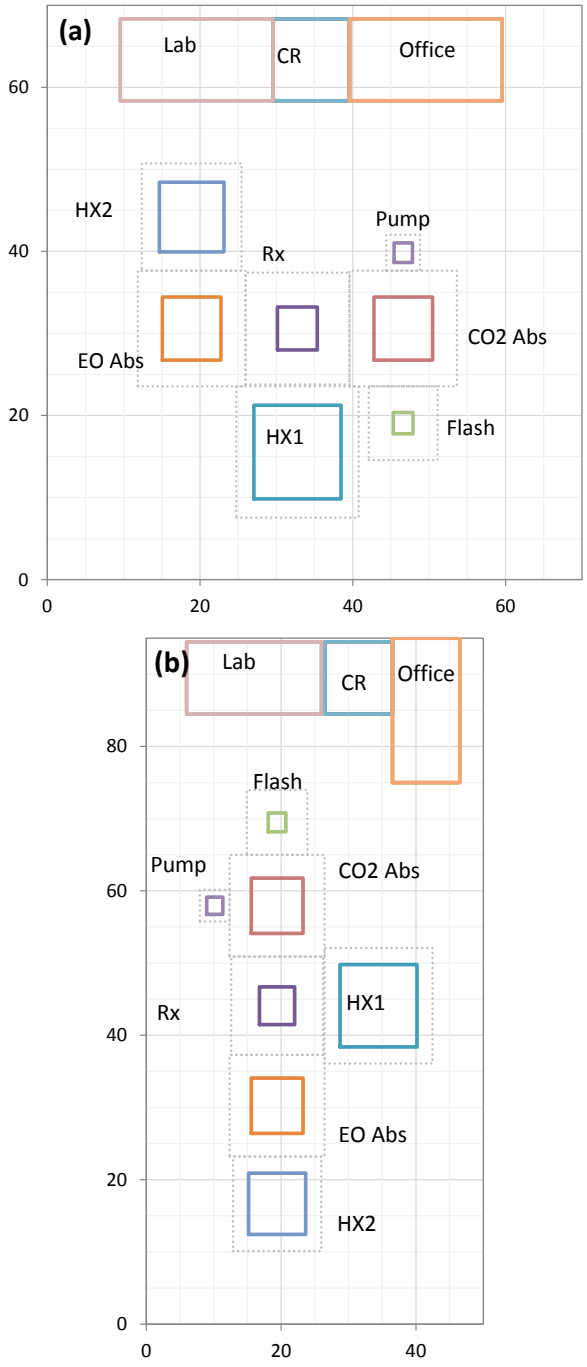

Figure 4.24 Optimal layout of EO plant in site option 1 with additional protective devices (a) square (b) rectangle.

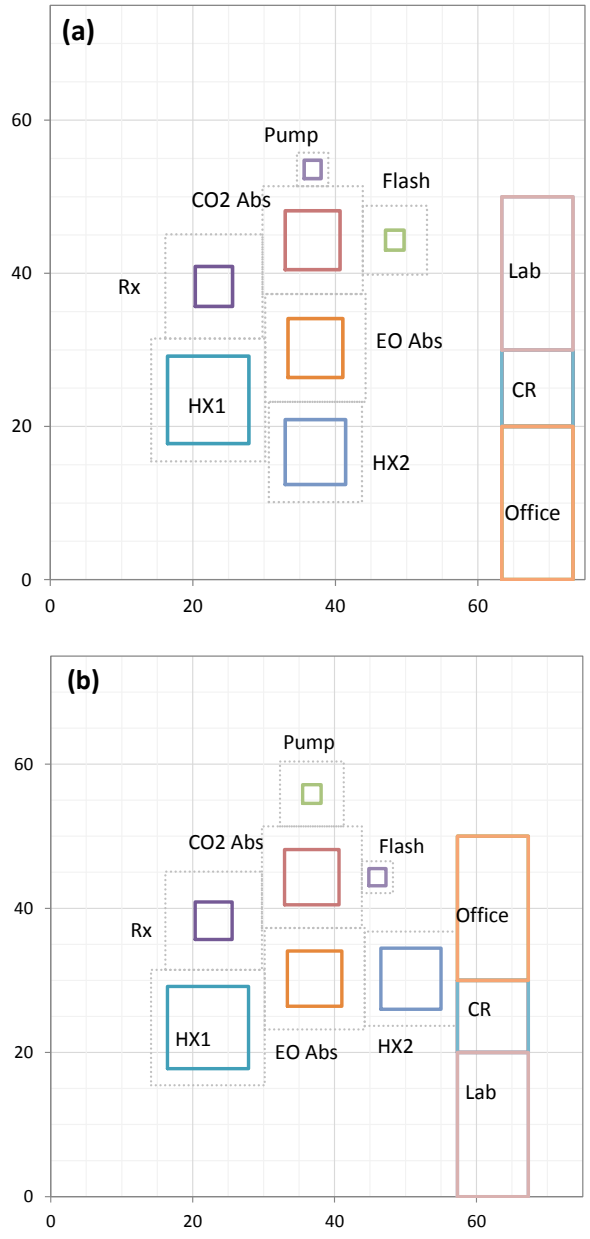

Figure 4.25 Optimal layout of EO plant in site option 2 with additional protective devices (a) square (b) rectangle.

Table 4.15 Layout result of EO plant with boundary factors and additional protective devices

		Option1		Option2	
Cost	Connection	21308	21308	22058	22058
[$]	Land	130340	126350	149625	149625
	Protection	40000	25000	10000	10000
	Total	191648	172658	181683	181683
Site	Shape	Square	Rectangle	Square	Square
	Width [m]	70	50	75	75
	Depth [m]	70	95	75	75
	Area [m^2]	4900	4750	5625	5625
Protective	Rx	K3	K3	K2	K2
device	EO Abs	K2	K2	K2	K2
configuration	CO2 Abs	K3	K2	K1	K1

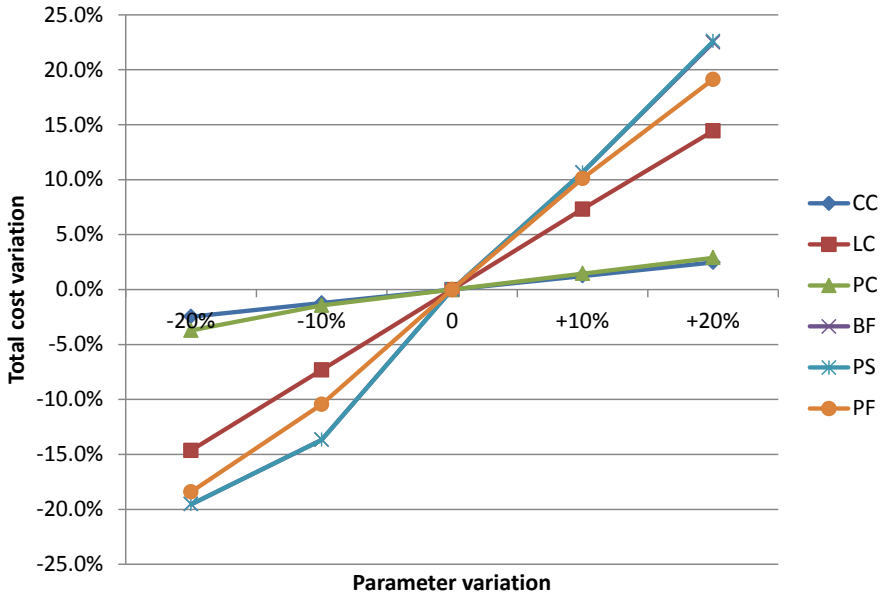

Figure 4.26 Parametric sensitivity for optimal layout of EO plant.

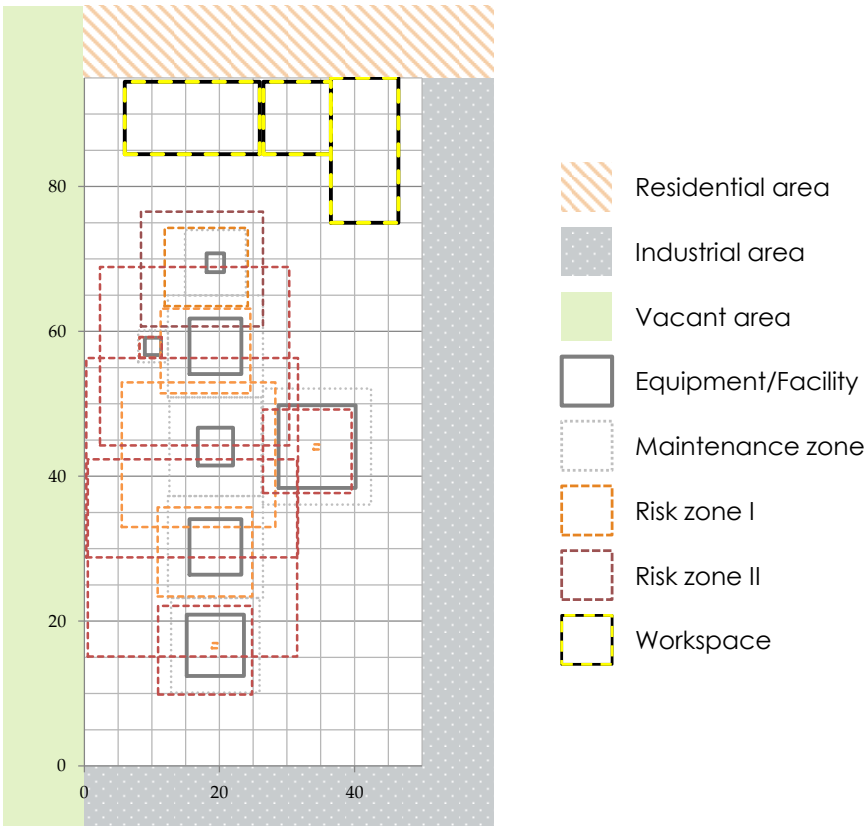

Figure 4.27 Risk zone representation for the optimal case.

The site selection problem can be further discussed. The process site in the urban area requires more land cost but can be more efficient in product transportation. On the other hand, if the process site is constructed in the suburb region, it would cost less for land purchase and social/environmental concerns. Since the relative positions of hazardous process equipment as well as the required land area can be distinguished for these cases, the proposed framework can support the decision between urban and suburb sites.

When it compared to the result of previous research, the proposed method demands larger land area. This is because the IR-based distance constraints are active for the boundaries of process site, while the conventional layout problem didn’t consider the spacing for boundaries. However, the process area, which is the smallest area containing process equipment, of the proposed result is 12% smaller than that of previous result due to the risk zone approach.

Table 4.16 Result comparison for layout of EO plant

	Patsiatzis (2004)	Proposed (with BF and PF)
Land area [m^2]	1,600	4,225
Relative value [%]	100	264
Process area [m^2]	1,600	1,406
Relative value [%]	100	88

4.3 Multi-floor layout optimization of liquefaction process of LNG FPSO

An FPSO (floating production, storage, and offloading) vessel is an integrated platform to process and store oil or gas while its offshore transportation from the resource fields to the consumption region. The pipelines or storage vessels without the production capability have been used to transport the hydrocarbons through the sea before this kind of facility. The FPSO is economically preferable since it replaces the requirement of pipeline and onshore production facility, and can move to the other resource field after the depletion [88].

One special type of FPSO for natural gas development is an LNG FPSO (liquefied natural gas FPSO) or FLNG (floating LNG) facility. Such floating plant for LNG is favorable because natural gas is a promising alternative energy resource to oil or coal, and most of its reserves are in distant, deep offshore fields [89], [90].

FPSO, including LNG FPSO, suffers from the restricted area since it is an offshore plant, and the pressurized equipment and flammability of natural gas make it vulnerable to the accident such as fire or explosion. However, there were not many studies for the systematic layout of process equipment in the FPSO although the

technologies for each module have been researched rigorously. Therefore, the proposed risk-based layout optimization framework has been applied to a part of the LNG FPSO to find out the safe and efficient layout.

The target of the layout optimization in this case study is a module in liquefaction process. The liquefaction process is a part of LNG FPSO located on the topside of the vessel, which consists of the process system and the utility system. In the process system, natural gas is processed through the separation, the pretreatment, and the fractionation processes, and then liquefied in the liquefaction process. Since the construction of the liquefaction process accounts nearly 30% of the total capital cost of an LNG FPSO, it is important to properly arrange the modules in the liquefaction process. Figure 4.28 depicts the composition of the capital cost of typical LNG FPSO [91].

Among several types of liquefaction cycles, the DMR (dual mixed refrigerant) process is regarded as the possible application to LNG FPSO since its high efficiency [91], [92]. In the DMR cycle, the refrigerant contains the mixture of methane, ethane, propane and butane is used in the main refrigeration and precooling section [93]–[95].

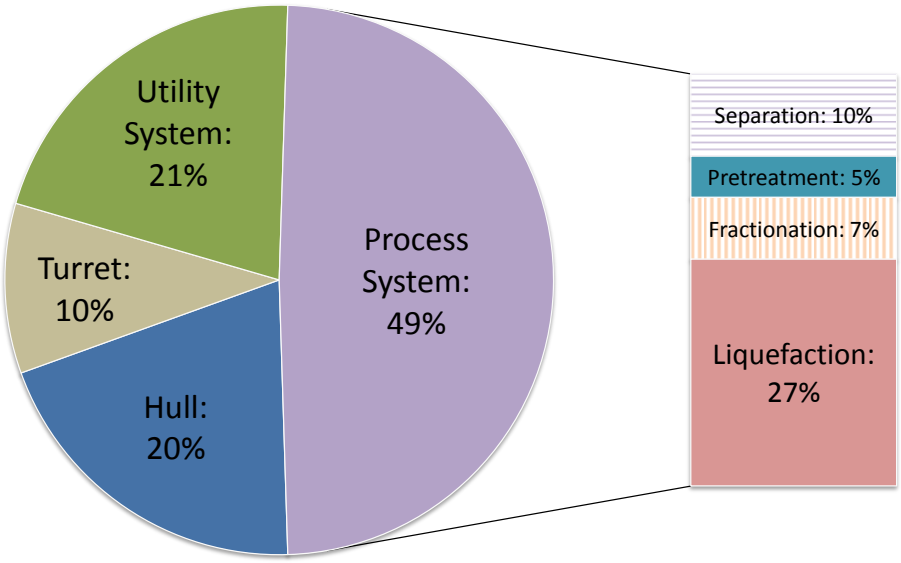

Figure 4.28 Breakdown of the capital cost of typical LNG FPSO.

4.3.1 Problem statement

In this study, the optimal layout of MR module of DMR cycle for the liquefaction process of LNG FPSO has been considered.

The DMR cycle of LNG liquefaction process consists of three modules – PMR (precooled mixed refrigerant) module 1, PMR module 2, and MR (mixed refrigerant) module [93]. The flow diagram of DMR cycle is depicted in Figure 4.29. Two PMR modules are not differentiated in this figure. In this study, the bottom part (MR module) is considered for the optimal layout.

The list of process equipment in MR module and their physical dimensions are shown in Table 4.17 [96]. There are five decks in the module and the height of a deck is assumed as 8 m, so the first three units cannot be contained in a single floor – MR separator and MR compressor suction drum requires two floors and MCHE (main cryogenic heat exchanger) takes up all five decks. Therefore, they are divided into smaller pieces no taller than 8 m. Total 16 equipment and their connectivity is presented in Table 4.18.

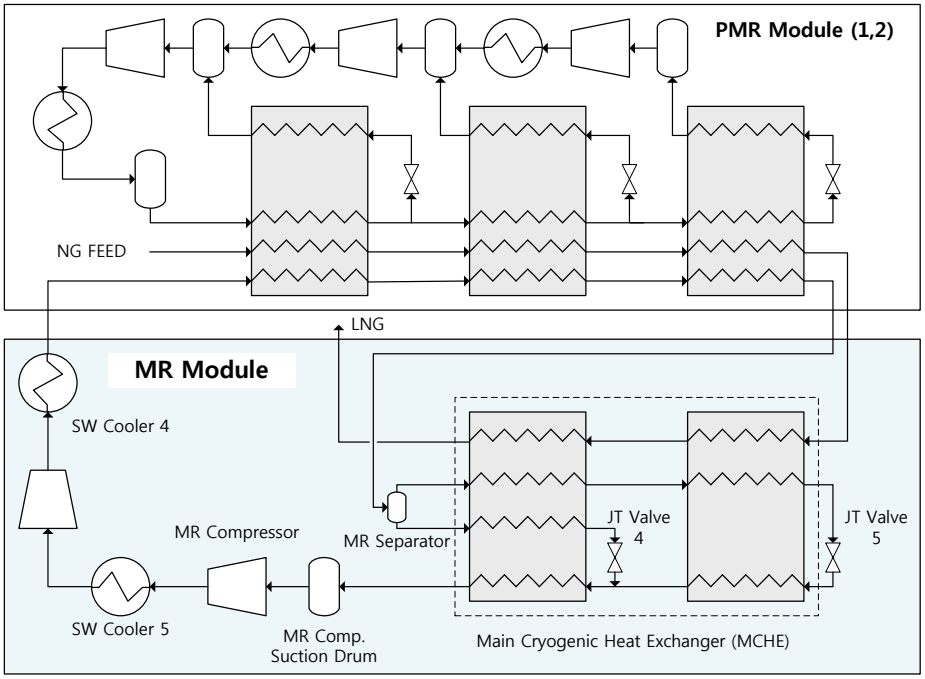

Figure 4.29 Module and equipment of DMR cycle.

Table 4.17 Equipment dimensions in MR module of DMR cycle

Equipment	Width [m]	Depth [m]	Height [m]
MR separator	4.24	4.24	12.25
MCHE	5.37	5.37	39.58
MR compressor suction drum	5.18	5.18	8.48
MR compressor	16.30	5.65	5.65
Cooler for compressor	2.83	1.88	2.83
Overhead crane	21.67	15.08	5.65
Sea water cooler 4	3.77	2.36	2.83
Sea water cooler 5	3.77	2.36	2.83
Joule-Thomson Valve 4	1.41	1.41	1.41
Joule-Thomson Valve 5	1.41	1.41	1.41

Table 4.18 Equipment information for multi-floor layout

ID	Equipment	Width [m]	Depth [m]	Height [m]	Connection
1	MR separator L	4.24	4.24	8.00	(1,4)
2	MR separator U	4.24	4.24	4.25	(4,15)
3	MCHE A	5.37	5.37	8.00	(15,4)
4	MCHE B	5.37	5.37	8.00	(2,5)
5	MCHE C	5.37	5.37	8.00	(5,6)
6	MCHE D	5.37	5.37	8.00	(6,16)
7	MCHE E	5.37	5.37	7.58	(16,7)
8	MR comp. suction drum L	5.18	5.18	8.00	(3,8)
9	MR comp. suction drum U	5.18	5.18	0.48	(9,10)
10	MR compressor	16.30	5.65	5.65	(10,13)
11	Cooler for comp.	2.83	1.88	2.83	(13,10)
12	Overhead crane	21.67	15.08	5.65	(10,14)
13	SW cooler 4	3.77	2.36	2.83	(10,11)
14	SW cooler 5	3.77	2.36	2.83	(11,10)
15	JT Valve 4	1.41	1.41	1.41	
16	JT Valve 5	1.41	1.41	1.41	

4.3.2 Formulation for multi-floor layout

Since the MR module of liquefaction process is designed in multiple floors, additional constraints are required to model the layout of equipment distributed or stretched over the multiple decks. The following constraints are brought from the work of Patsiatzis [23].

First, a binary variable is introduced for the assignment of equipment on one floor.

$$\sum_{f} V_{if} = 1 \tag{4.5}$$

Another binary variable becomes 1 if two units are allocated on the same floor, otherwise, 0.

$$Z_{ij} \geq V_{if} + V_{jf} - 1 \tag{4.6}$$

$$Z_{ij} \leq 1 - V_{if} + V_{jf} \tag{4.7}$$

$$Z_{ij} \leq 1 + V_{if} - V_{jf} \tag{4.8}$$

$$\forall\, i = 1, \dots, N-1,\ \ \forall\, j = i+1,\ \ \dots, N, \forall f = 1, \dots, F$$

The distance in vertical direction is also included.

$$U_{ij} - D_{ij} = FH \sum_{f} f\left(V_{if} - V_{jf}\right) + z_i - z_j \tag{4.9}$$

Then, the total rectilinear distance between equipment (Equation (3.22)) becomes:

$$TD_{ij} = R_{ij} + L_{ij} + A_{ij} + B_{ij} + U_{ij} + D_{ij} \tag{4.10}$$

The non-overlapping constraints need to be activated only if the equipment is on the same floor. Therefore, (3.23)-(3.26) should be replaced as follows.

$$x_i - x_j + M\left(1 - Z_{ij} + E1_{ij} + E2_{ij}\right) \geq \frac{l_i + l_j}{2} \tag{4.11}$$

$$x_j - x_i + M\left(2 - Z_{ij} - E1_{ij} + E2_{ij}\right) \geq \frac{l_i + l_j}{2} \tag{4.12}$$

$$y_i - y_j + M\left(2 - Z_{ij} + E1_{ij} - E2_{ij}\right) \geq \frac{d_i + d_j}{2} \tag{4.13}$$

$$y_j - y_i + M\left(3 - Z_{ij} - E1_{ij} - E2_{ij}\right) \geq \frac{d_i + d_j}{2} \tag{4.14}$$

$$\forall\, i = 1, \dots, N-1, \qquad \forall\, j = i+1, \dots, N$$

In addition to these ‘general’ equations for the multi-floor layout problem, some specific constraints are required for this case study [97].

(1) Equipment stretched multiple decks

MR separator, MCHE and MR compressor suction drum are divided into smaller pieces but they are physically the same unit. Therefore, the coordinate of the center of them should be the same. Moreover, the binary variable for floor allocation (V) for them must be 1 for consecutive floors.

(2) Related equipment

MR compressor, cooler for compressor and the overhead crane is closely related to. Their x- and y-coordinates should coincide and the value of V for them must be 1 for consecutive floors.

General layout problem considers the pumping cost for the vertical pipeline. In LNG FPSO, however, it is not necessary because all the flow has high pressure already. Moreover, the number of the decks in the liquefaction process is fixed. Therefore, the objective function remains the same.

4.3.3 Risk calculation

The modified individual risks of the process equipment of the MR module are calculated from the frequency and the consequence analysis results of the possible hazards.

Vapor cloud explosion (VCE), flash fire and jet fire were identified as the possible hazards. Using the failure rate data and event tree analysis (ETA), the frequencies of each accident scenario for all the equipment were obtained. Then, consequences, i.e. the overpressure from VCE and thermal radiation from the fires were calculated by using the known empirical equations.

The individual risks depending on the distances from the centers of the process equipment are presented in Figure 4.30. For this particular case study, tightened criteria of IR are used: the IR at required spacing for workers should be less than 10^{-5} per annum and for the public should be less than 10^{-6} per annum. Such spacing values and the IR at those distances are listed in Table 4.19. The separation distance between equipment used the value of 4 m.

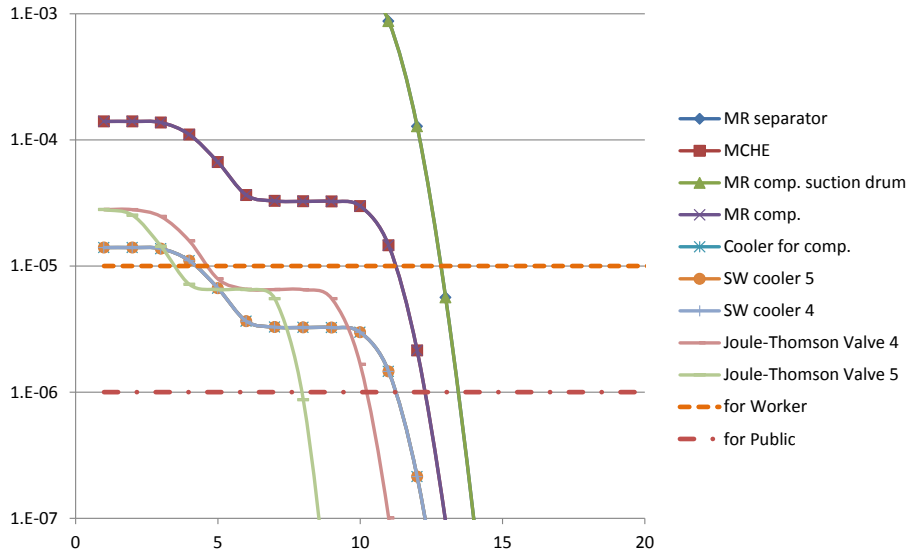

Figure 4.30 IR of equipment in MR module of DMR process.

Table 4.19 Required spacing based on IR of equipment

Equipment	For worker		For the public	
	WS [m]	IR [10^{-5}yr^{-1}]	PS [m]	IR [10^{-6}yr^{-1}]
MR separator	13	0.56	14	0.094
MCHE	12	0.21	13	0.094
MR comp. suction drum	13	0.56	14	0.094
MR comp.	12	0.21	13	0.094
Cooler for comp.	5	0.67	12	0.21
SW cooler 4	5	0.67	12	0.21
SW cooler 5	5	0.67	12	0.21
Joule-Thomson Valve 4	5	0.79	11	0.10
Joule-Thomson Valve 5	4	0.72	8	0.87

In LNG FPSO, it is not reasonable to assume the surrounding residential areas. The living quarters for workers are also located in distant part of the vessel. Instead, a side of MR module should be uncovered for maintenance purpose [97]. Therefore, it is assumed that the north boundary of MR module is workspace, the west and east boundary is industrial area, and the south boundary is sea (vacant).

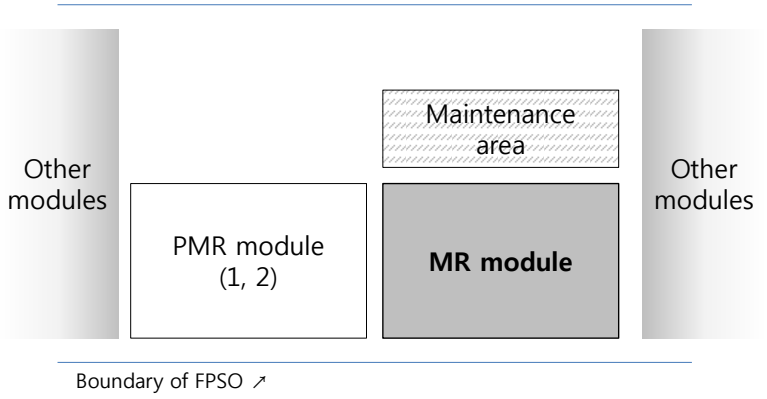

Figure 4.31 Assumption of surrounding circumstances of MR module of DMR cycle in LNG FPSO.

4.3.4 Layout result and discussion

Three cases have been considered for the layout optimization of MR module of DMR cycle. To prevent the problem is being too complicated, the problems are solved only for the rectangular floor area.

There were no additional restrictions other than the constraints in previous section for the first one. The layout results are presented in Figure 4.32 as the top view of each deck, and as the 3-D view in Figure 4.33. As can be seen the figure, the shape of floor area is horizontally long rectangle. Since there are many other modules in the LNG FPSO, this kind of shape of module might not be efficient to allocate the other modules. Therefore, the next problem is considered.

(Deck A)

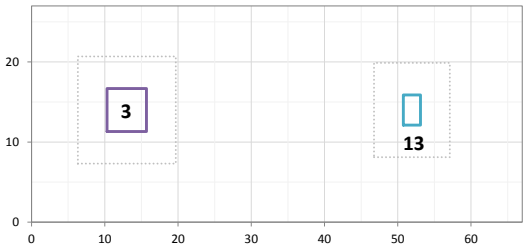

(Deck B)

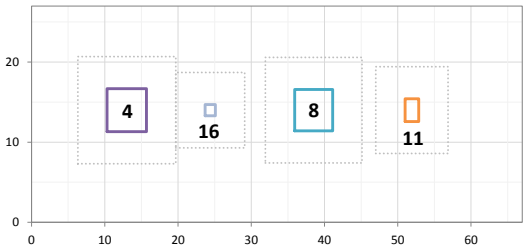

(Deck C)

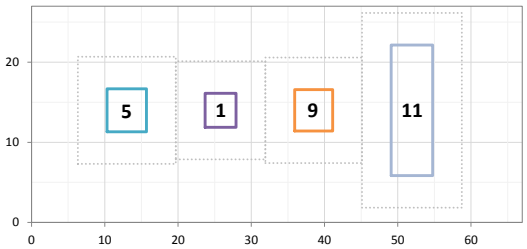

(Deck D)

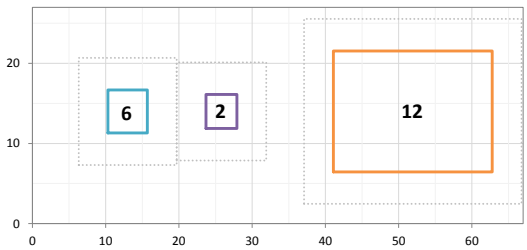

(Deck E)

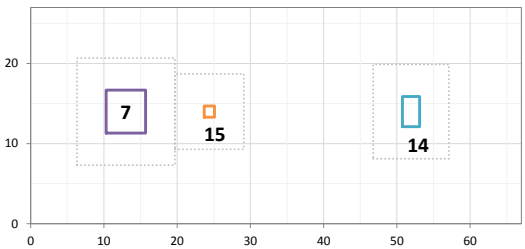

Figure 4.32 Optimal layout of MR module of DMR cycle.

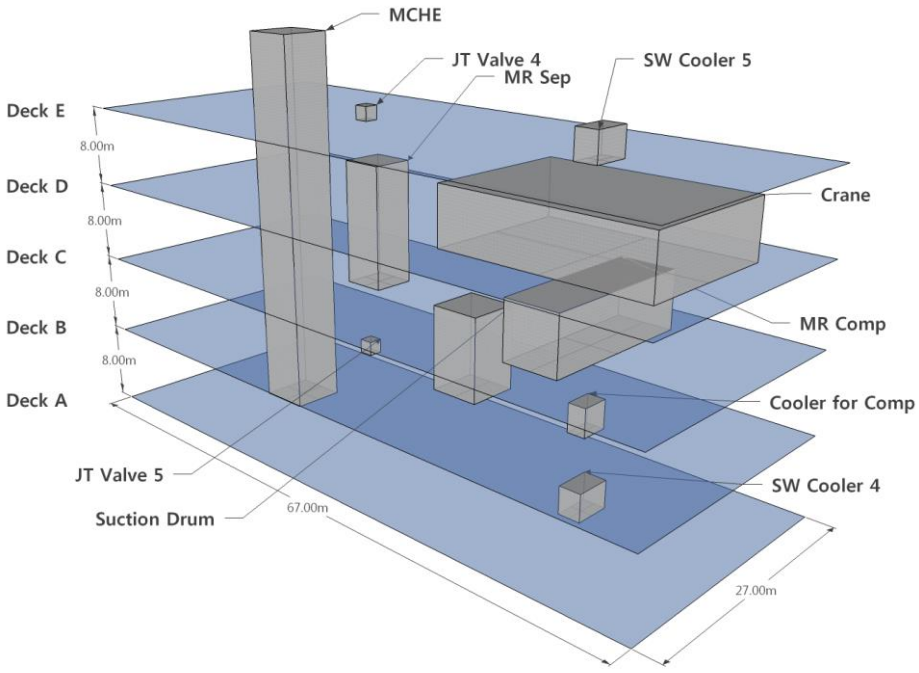

Figure 4.33 Optimal layout of MR module of DMR cycle (3-D).

In the second case, the ratio of the width and the depth of the floor area are restricted under 1.5. That is, width should be smaller than 1.5 x depth. The result was slight increase in the total cost due to the enlarged floor area. However, this case might be beneficial if the allocation of modules is considered. The plane view and the 3-D view of layout result are illustrated in Figure 4.34 and Figure 4.35.

The final case considered the boundary factors. As mentioned in the previous section, the residential area is ignored. Figure 4.36 and Figure 4.37 are the layout result of this case. The cost of layout for this case was lower than that of former cases since the required spacing is smaller.

The detailed cost and the site dimension result can be found in Table 4.20.

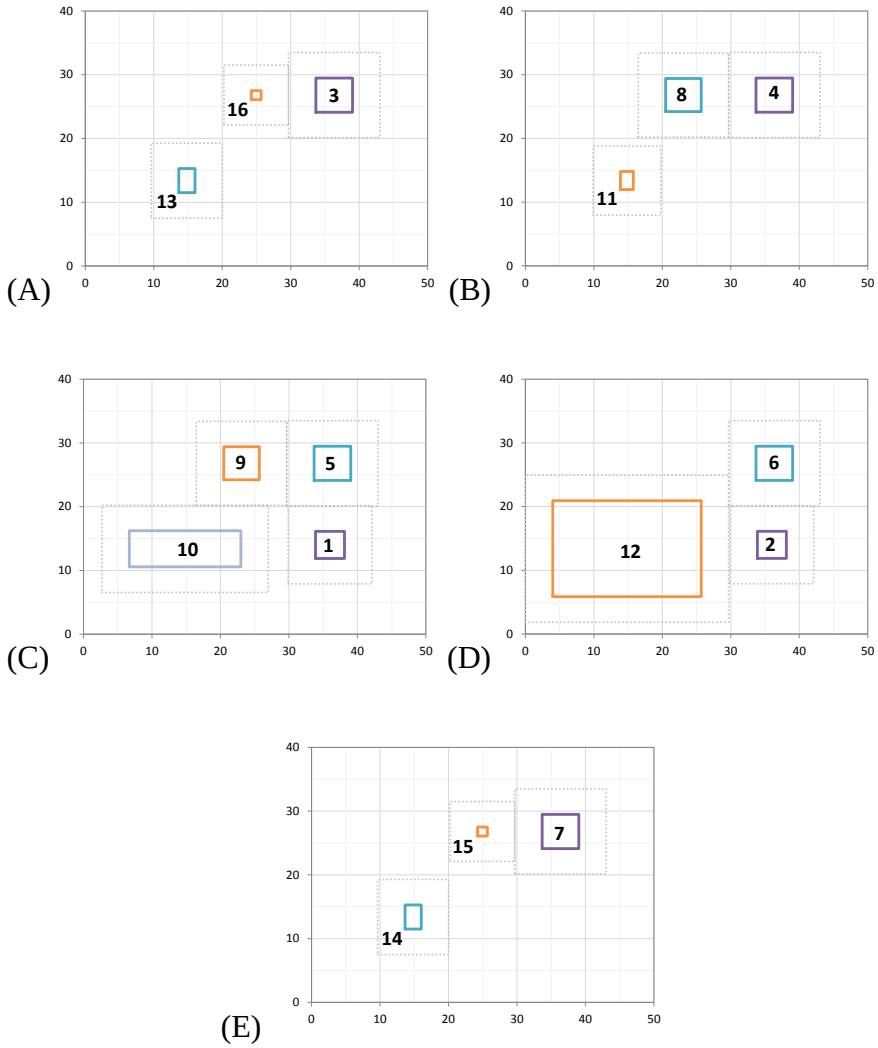

Figure 4.34 Optimal layout of MR module of DMR cycle with ratio restriction.

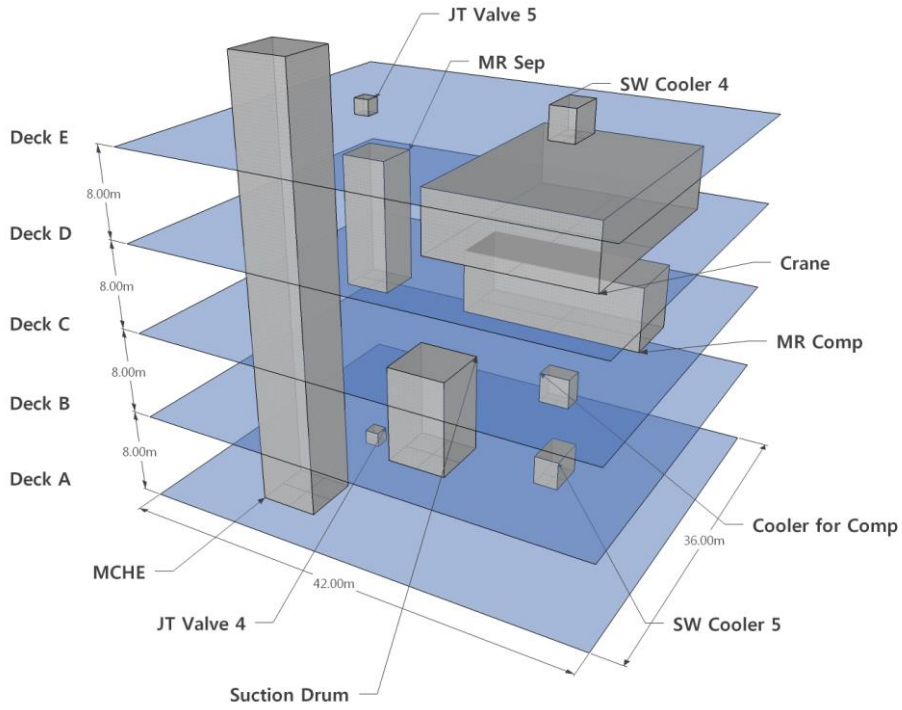

Figure 4.35 Optimal layout of MR module of DMR cycle with ratio restriction (3-D).

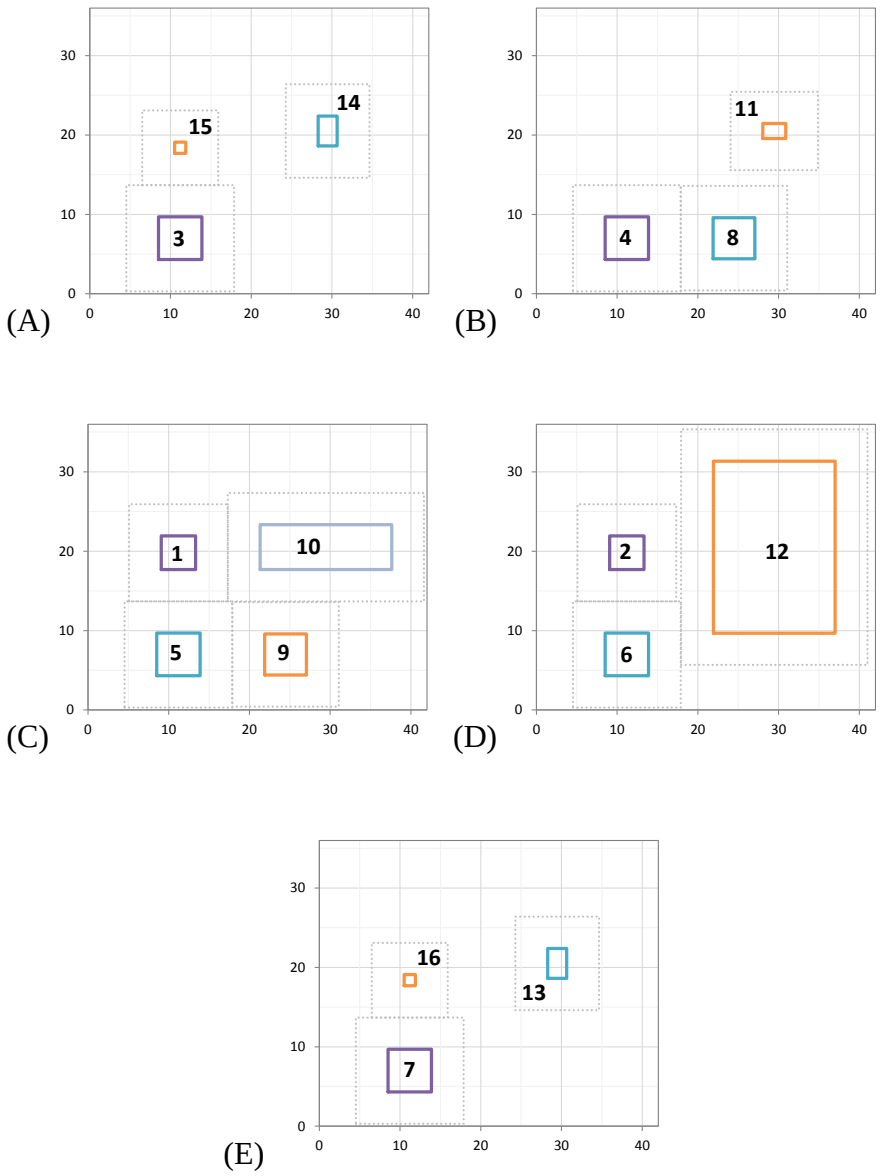

Figure 4.36 Optimal layout of MR module of DMR cycle with boundary factors.

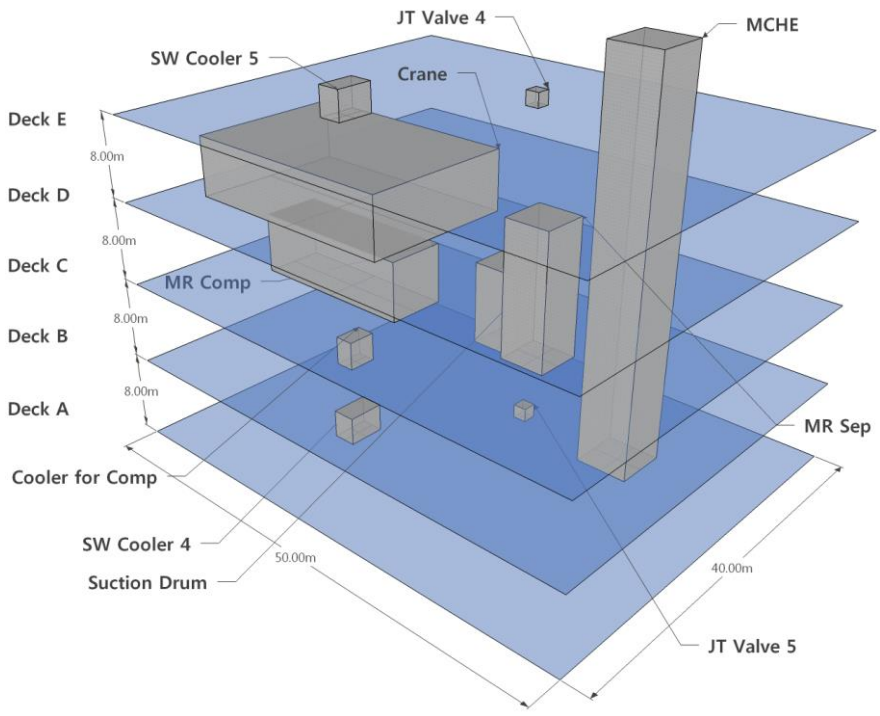

Figure 4.37 Optimal layout of MR module of DMR cycle with boundary factors (3-D).

Table 4.20 Layout results of MR module

	Cost			Site		
	Connect [rmu]	Floor [rmu]	Total [rmu]	Width [m]	Depth [m]	Area [m^2]
Base	292.9	48119	48412	67	27	1809
Ratio restriction	284.1	53200	53484	50	40	2000
BF	273.8	40219	40493	42	36	1512

5 Conclusion

A chemical process plant deals with the hazardous materials in dangerous operation conditions always have the risk of accident such as fire and explosion. In order to prevent such risk to be realized, there have been many researches related to the proper layout of the chemical processes. The major goals, however, were the enhancement of economic efficiency or the decrease of the possible loss. Although both objectives are also crucial, one can say that securing the safety for humans is the most important thing.

To minimize the risk to humans in the layout of chemical processes, this thesis addressed the modified individual risk (IR) - based layout optimization methodology. IR from the process equipment is assessed from the frequency and consequence analysis result to express the possible risk from the process to nearby humans including workers and the public. Then, the risk zones were constructed from the safety distances for humans, which were converted from IR. The MILP formulation for process layout optimization was carried out including the constraints for the minimization of risks to people such as non-overlapping constraints of these risk zones, boundary land use factor, and additional

protective device installation. In the solution stage, iterative search procedure was applied to tackle the layout problem with large number of process equipment.

The proposed methodology was applied to three chemical processes. The first one was a dimethyl ether (DME) filling station which has small number of equipment. The capacity distribution case was examined to find the optimal point of equipment combinations. The second application was an ethylene oxide (EO) plant. For that case, the decision making of construction site selection was considered under the different boundary land uses. A module in the liquefaction process of liquefied natural gas (LNG) floating production, storage, offloading (FPSO) vessel was considered last. The arrangement of process equipment was carried out on multiple decks. Throughout these case studies, the applicability of the proposed framework and its solution efficiency was verified.

This thesis developed a new framework of layout optimization based on the well-known quantitative risk assessment, and has its own benefits.

- The proposed method can create the optimal layout of chemical processes minimizing the risk to nearby people, and map the risk level as the risk contour or risk zones.

This risk-based process layout can provide the inherent safety of the process in the early stage of process design.

- The risk zone representation reduces the required site area for the same separation distances, so the total cost of layout can be reduced.
- The proposed method can provide the support for the decision making related with the process layout such as the allocation of process site or the installation of additional protective devices.
- Iterative search procedure included in the solution stage provides efficiency under the complex conditions for the risk considerations.
- Some practical applications have been dealt with. In particular, the layout of the liquefaction process of a LNG FPSO, which caught attention from both academic and industrial point of view, was arranged including risk consideration.

Some topics or directions recommended for further study from this thesis is as follows:

- The conversion of IR to the safety distance and the risk zone is conducted by the ‘threshold-like’ manner in this

study. Instead, mapping the IR as a function of the distance from the hazards and include it (or its transformation) in the objective function can provide the further possibility of multi-objective optimization.

- Assessment of IR for certain points in the process site can lead to more accurate risk consideration. Grid (or cell) representation might be helpful.
- In the multi-floor application, the risk zones can be expanded to a cube or other three dimensional shape. By doing so, the risks between floors can be counted.
- Many process layout problems occur when the expansion is planned for the chemical plant. The allocation of additional equipment/facilities in the existing chemical process plant can be a practical application based on the proposed methodology. In that case, the minimization of the risk in the objective function rather than the limitation of the risk by the constraints might be preferred due to the risks from existing equipment.

Nomenclatures

Sets

f	Floor number
i, j	Process equipment
k	Group of people
p	Protective device
s ($s1$, $s2$)	Candidate of square (rectangular) process site
u	Location or equipment of interest
v	Event outcome

Parameters

a_i, b_i	Length of each side of i
AR_s	Land area of s
BF	Boundary land use factor (direction-wise)
C_i^{eq}	Purchase cost of i
C^{land}	Unit cost of land area
C_{ij}^{pipe}	Unit cost of pipeline connected between i and j
C_i^{prot}	Cost of protective device installed on i
CN_{ij}	Connectivity between i and j
ES_i	Equipment spacing distance of i

$f_{eo,v}$	Frequency of *v*
FH	Floor height
FoF_u	Frequency of fatality at *u*
$IR_{u,k}$	Individual risk of fatality to *k* at *u*
$IR_{u,v}$	Individual risk of fatality to *u* from *v*
M	Appropriate large number ("big-M")
N	Total number of equipment
NF	Number of floors
$p_{u,v}^{\mathrm{dir}}$	Probability of *v* being directed at *u*
$p_{u,v}^{\mathrm{fat}}$	Probability of fatality at *u* produced by *v*
$p_{u,k}^{\mathrm{loc}}$	Probability of *k* is located at *u*
$p_{u,v}^{\mathrm{wea}}$	Probability of the weather condition required to produce *v* at *u*
PF_p	Risk protection factor of *p*
PS_i	Risk boundary distance for public people from *i*
wid_s (dep_s)	Width (Depth) of *s*
WS_i	Risk boundary distance for workspace from *i*
θ_k	Fraction of time that *k* spends in the area of interest

Variables

A_{ij}(B_{ij})	Distance in y-axis between the center of *i* and *j*
$E1_{ij}, E2_{ij}$	Binary variables for non-overlapping constraints

l_i (d_i)	Horizontal (Vertical) length of *i*
LA (FA)	Land (floor) area of process site
O_i	Binary variable for orientation of *i*
$PI_{i,p}$	Binary variable for installation of *p* on *i*
Q_s	Selection of *s*
R_{ij} (L_{ij})	Distance in x-axis between the center of *i* and *j*
TD_{ij}	Total rectilinear distance between *i* and *j*
U_{ij} (D_{ij})	Distance in z-axis between the center of *i* and *j*
$V_{i,f}$	Binary variable for existence of *i* at *f*
$x^{\max}$ $(y^{\max})$	Length in *x*- (*y*-) direction of process site
x_i (y_i)	*x*- (*y*-) coordinate of center of *i*
Z_{ij}	Binary variable. 1 if *i* and *j* are located on the same *f*
z_i	Height of connection of *i*

Abbreviations

BLEVE	Boiling liquid expanding vapor explosion
DME	Dimethyl ether
(D)MR	(Dual) Mixed refrigerant
EO	Ethylene oxide
FPSO	Floating production, storage and offloading (vessel)
GTL	Gas-to-liquid
IR	Individual risk

JT valve	Joule-Thomson valve
LNG	Liquefied natural gas
LPG	Liquefied petroleum gas
MCHE	Main cryogenic heat exchanger
MILP	Mixed integer linear programming
MINLP	Mixed integer non-linear programming
PMR	Precooled mixed refrigerant
QRA	Quantitative risk assessment (or analysis)
rmu	Relative monetary unit
RPLO	Risk-based process layout optimization
SW cooler	Seawater cooler
TNT	Trinitrotoluene
VCE	Vapor cloud explosion

References

[1] C. M. Pietersen, “Analysis of the LPG-disaster in mexico city,” *J. Hazard. Mater.*, **20**, 85–107, 1988.

[2] K. Park, M. Sam Mannan, Y.-D. Jo, J.-Y. Kim, N. Keren, and Y. Wang, “Incident analysis of Bucheon LPG filling station pool fire and BLEVE,” *J. Hazard. Mater.*, **137**(1), 62–67, 2006.

[3] F. I. Khan and P. R. Amyotte, “Modeling of BP Texas City refinery incident,” *J. Loss Prev. Process Ind.*, **20**(4–6), 387–395, 2007.

[4] S. B. Park, “Alert over South Korea toxic leaks,” *Nature*, **494**(7435), 15–16, 2013.

[5] “West Fertilizer Company explosion,” *Wikipedia, the free encyclopedia*. 2013.

[6] J. C. Mecklenburgh, *Process plant layout*. John Wiley and Sons, Inc.,New York, NY, 1985.

[7] Center for Chemical Process Safety, *Guidelines for Chemical Process Quantitative Risk Analysis*, 2nd ed. New York: Wiley-AIChE, 1999.

[8] J. M. Moore, *Plant layout and design*. Prentice Hall, 1962.

[9] J. C. Mecklenburgh, *Plant layout: a guide to the layout of process plant and sites*. New York: Wiley, 1973.

[10] A. Suzuki, T. Fuchino, M. Muraki, and T. Hayakawa, “An Evolutionary Method of Arranging the Plot Plan for Process Plant Layout,” *J. Chem. Eng. Jpn.*, **24**(2), 226–231, 1991.

[11] S. Abdinnour-Helm and S. W. Hadley, “Tabu search based heuristics for multi-floor facility layout,” *Int. J. Prod. Res.*, **38**(2), 365–383, 2000.

[12] M. M. Hassan and G. L. Hogg, “A review of graph theory application to the facilities layout problem,” *Omega*, **15**(4), 291–300, 1987.

[13] S. Jayakumar and G. V. Reklaitis, “Chemical plant layout via graph partitioning-1. Single level,” *Comput. Chem. Eng.*, **18**(5), 441–458, 1994.

[14] S. Jayakumar and G. V. Reklaitis, “Chemical plant layout via graph partitioning—II. Multiple levels,” *Comput. Chem. Eng.*, **20**(5), 563–578, 1996.

[15] K. H. Watson and J. W. Giffin, “The Vertex Splitting Algorithm for facilities layout,” *Int. J. Prod. Res.*, **35**(9), 2477–2492, 1997.

[16] L. R. Foulds, H. W. Hamacher, and J. M. Wilson, “Integer programming approaches tofacilities layout models with forbidden areas,” *Ann. Oper. Res.*, **81**(0), 405–418, 1998.

[17] M. C. Georgiadis and S. Macchietto, “Layout of process plants: A novel approach,” *Comput. Chem. Eng.*, **21**, S337–S342, 1997.

[18] M. C. Georgiadis, G. E. Rotstein, and S. Macchietto, “Optimal Layout Design in Multipurpose Batch Plants,” *Ind. Eng. Chem. Res.*, **36**(11), 4852–4863, 1997.

[19] M. C. Georgiadis, G. Schilling, G. E. Rotstein, and S. Macchietto, “A general mathematical programming approach for process plant layout,” *Comput. Chem. Eng.*, **23**(7), 823–840, 1999.

[20] A. P. Barbosa Póvoa and S. Macchietto, “Optimal design of multipurpose batch plants 1. Problem formulation,” *Comput. Chem. Eng.*, **17, Supplement 1**, S33–S38, 1993.

[21] A. P. Barbosa-Póvoa and S. Macchietto, “Detailed design of multipurpose batch plants,” *Comput. Chem. Eng.*, **18**(11–12), 1013–1042, 1994.

[22] L. G. Papageorgiou and G. E. Rotstein, “Continuous-Domain Mathematical Models for Optimal Process Plant Layout,” *Ind. Eng. Chem. Res.*, **37**(9), 3631–3639, 1998.

[23] D. I. Patsiatzis and L. G. Papageorgiou, “Optimal multi-floor process plant layout,” *Comput. Chem. Eng.*, **26**(4–5), 575–583, 2002.

[24] J. Westerlund, L. G. Papageorgiou, and T. Westerlund, “A MILP model for N-dimensional allocation,” *Comput. Chem. Eng.*, **31**(12), 1702–1714, 2007.

[25] K. Park, J. Koo, D. Shin, C. J. Lee, and E. S. Yoon, “Optimal multi-floor plant layout with consideration of safety distance based on mathematical programming and modified consequence analysis,” *Korean J. Chem. Eng.*, **28**(4), 1009–1018, 2011.

[26] D. I. Patsiatzis, G. Knight, and L. G. Papageorgiou, “An MILP Approach to Safe Process Plant Layout,” *Chem. Eng. Res. Des.*, **82**(5), 579–586, 2004.

[27] G. Xu and L. G. Papageorgiou, “A Construction-Based Approach to Process Plant Layout Using Mixed-Integer Optimization,” *Ind. Eng. Chem. Res.*, **46**(1), 351–358, 2007.

[28] G. Xu and L. G. Papageorgiou, “Process plant layout using an improvement-type algorithm,” *Chem. Eng. Res. Des.*, **87**(6), 780–788, 2009.

[29] R. Guirardello and R. E. Swaney, “Optimization of process plant layout with pipe routing,” *Comput. Chem. Eng.*, **30**(1), 99–114, 2005.

[30] W. Xie and N. V. Sahinidis, “A branch-and-bound algorithm for the continuous facility layout problem,” *Comput. Chem. Eng.*, **32**(4–5), 1016–1028, 2008.

[31] F. D. Penteado and A. R. Ciric, “An MINLP Approach for Safe Process Plant Layout,” *Ind. Eng. Chem. Res.*, **35**(4), 1354–1361, 1996.

[32] I. Castillo, J. Westerlund, S. Emet, and T. Westerlund, “Optimization of block layout design problems with unequal areas: A comparison of MILP and MINLP optimization methods,” *Comput. Chem. Eng.*, **30**(1), 54–69, 2005.

[33] I. Castillo and T. Westerlund, “An ε-accurate model for optimal unequal-area block layout design,” *Comput. Oper. Res.*, **32**(3), 429–447, 2005.

[34] S. Lee and I. E. Grossmann, “New algorithms for nonlinear generalized disjunctive programming,” *Comput. Chem. Eng.*, **24**(9–10), 2125–2141, 2000.

[35] I. E. Grossmann, “Review of Nonlinear Mixed-Integer and Disjunctive Programming Techniques,” *Optim. Eng.*, **3**(3), 227–252, 2002.

[36] I. E. Grossmann and J. P. Ruiz, “Generalized Disjunctive Programming: A Framework for Formulation and Alternative Algorithms for MINLP Optimization,” in *Mixed Integer Nonlinear Programming*, J. Lee and S. Leyffer, Eds. Springer New York, 2012, 93–115.

[37] C. Díaz-Ovalle, R. Vázquez-Román, and M. Sam Mannan, “An approach to solve the facility layout problem based on the worst-case scenario,” *J. Loss Prev. Process Ind.*, **23**(3), 385–392, 2010.

[38] S. Jung, D. Ng, J.-H. Lee, R. Vazquez-Roman, and M. S. Mannan, “An approach for risk reduction (methodology) based on optimizing the facility layout and siting in toxic gas release scenarios,” *J. Loss Prev. Process Ind.*, **23**(1), 139–148, 2010.

[39] R. Vázquez-Román, J.-H. Lee, S. Jung, and M. S. Mannan, “Optimal facility layout under toxic release in process facilities: A stochastic approach,” *Comput. Chem. Eng.*, **34**(1), 122–133, 2010.

[40] R. Vazquez-Roman and M. S. Mannan, “A New Trend in Designing Plant Layouts for the Process Industry,” in *Modeling Simulation and Optimization - Tolerance and Optimal Control*, InTech, 2010.

[41] C. O. Diaz, R. Vázquez-Román, S. Jung, and M. S. Mannan, “A Comparison of Deterministic and Stochastic Approaches to Solve the Facility Layout Problem with Toxic Releases,” in *Computer Aided Chemical Engineering*, **Volume 26**, Jacek Jeżowski and Jan Thullie, Ed. Elsevier, 2009, 93–98.

[42] S. P. Singh and R. R. K. Sharma, “A review of different approaches to the facility layout problems,” *Int. J. Adv. Manuf. Technol.*, **30**(5–6), 425–433, 2006.

[43] D. M. Tate and A. E. Smith, “Unequal-area facility layout by genetic search,” *Iie Trans.*, **27**(4), 465–472, 1995.

[44] T. D. Mavridou and P. M. Pardalos, “Simulated Annealing and Genetic Algorithms for the Facility Layout Problem: A Survey,” in *Computational Issues in High Performance Software for Nonlinear Optimization*, A. Murli and G. Toraldo, Eds. Springer US, 1997, 111–126.

[45] C. M. L. Castell, R. Lakshmanan, J. M. Skilling, and R. Bañares-Alcántara, “Optimisation of process plant layout using genetic algorithms,” *Comput. Chem. Eng.*, **22, Supplement 1**, S993–S996, 1998.

[46] F. Azadivar and J. Wang, “Facility layout optimization using simulation and genetic algorithms,” *Int. J. Prod. Res.*, **38**(17), 4369–4383, 2000.

[47] Industrial Risk Insurers Information, “PLANT LAYOUT AND SPACING FOR OIL AND CHEMICAL PLANTS,” I.M.2.5.2, 1991.

[48] G. Walker, “Land use planning, industrial hazards and the ‘COMAH’ Directive,” *Land Use Policy*, **12**(3), 187–191, 1995.

[49] G. M. . Laheij, J. . Post, and B. J. . Ale, “Standard methods for land-use planning to determine the effects on societal risk,” *J. Hazard. Mater.*, **71**(1–3), 269–282, 2000.

[50] U. Hauptmanns, “A risk-based approach to land-use planning,” *J. Hazard. Mater.*, **125**(1–3), 1–9, 2005.

[51] S. Jung, D. Ng, C. D. Laird, and M. S. Mannan, “A new approach for facility siting using mapping risks on a plant grid area and optimization,” *J. Loss Prev. Process Ind.*, **23**(6), 824–830, 2010.

[52] D. B. Özyurt and M. J. Realff, “Geographic and process information for chemical plant layout problems,” *Aiche J.*, **45**(10), 2161–2174, 1999.

[53] D. I. Patsiatzis and L. G. Papageorgiou, “Efficient Solution Approaches for the Multifloor Process Plant Layout Problem,” *Ind. Eng. Chem. Res.*, **42**(4), 811–824, 2003.

[54] G. Xu and L. G. Papageorgiou, “An iterative solution approach to process plant layout using mixed integer optimisation,” in *Computer Aided Chemical Engineering*, **Volume 24**, Valentin Pleşu and Paul Şerban Agachi, Ed. Elsevier, 2007, 419–424.

[55] L. Y. Liang and W. C. Chao, “The strategies of tabu search technique for facility layout optimization,” *Autom. Constr.*, **17**(6), 657–669, 2008.

[56] American Institute of Chemical Engineers, *Dow’s Fire & Explosion Index Hazard Classification Guide*, 7th ed. New York: Wiley-AIChE, 1994.

[57] D. J. Ball and S. Boehmer-Christiansen, “Societal concerns and risk decisions,” *J. Hazard. Mater.*, **144**(1–2), 556–563, 2007.

[58] D. Lisbona, J. Januszewski, H. Balmforth, and M. Wardman, “Societal risk assessment of major hazard installations using QuickRisk,” *Process Saf. Environ. Prot.*, **89**(6), 404–414, 2011.

[59] F. O. Moura Carneiro, H. H. Barbosa Rocha, and P. A. Costa Rocha, “Investigation of possible societal risk associated with wind power generation systems,” *Renew. Sustain. Energy Rev.*, **19**, 30–36, 2013.

[60] I. L. Hirst and D. A. Carter, “A ‘worst case’ methodology for obtaining a rough but rapid indication of the societal risk from a major accident hazard installation,” *J. Hazard. Mater.*, **92**(3), 223–237, 2002.

[61] Amey VECTRA Limited, “A Simplified Approach to Estimating Individual Risk,” Health and Safety Executive, 2007.

[62] Health and Safety Executive, *Reducing risks, protecting people*. HSE Books, 2001.

[63] D. J. Smith, *RELIABILITY, MAINTAINABILITY AND RISK: PRACTICAL SAFETY-RELATED SYSTEMS ENGINEERING METHODS*, 8th ed. Elsevier, 2011.

[64] R. F. Stapelberg, *Handbook of Reliability, Availability, Maintainability and Safety in Engineering Design*. Springer, 2008.

[65] Y.-D. Jo and D. A. Crowl, "Individual risk analysis of high-pressure natural gas pipelines," *J. Loss Prev. Process Ind.*, **21**(6), 589–595, 2008.

[66] T. Abbasi and S. Abbasi, "The boiling liquid expanding vapour explosion (BLEVE): Mechanism, consequence assessment, management," *J. Hazard. Mater.*, **141**(3), 489–519, 2007.

[67] R. W. Prugh, "Quantitative Evaluation of 'Bleve' Hazards," *J. Fire Prot. Eng.*, **3**(1), 9–24, 1991.

[68] M. J. Assael and K. E. Kakosimos, *Fires, Explosions, and Toxic Gas Dispersions: Effects Calculation and Risk Analysis*. CRC Press, 2010.

[69] K. Van Wingerden, O. R. Hansen, and P. Foisselon, "Predicting blast overpressures caused by vapor cloud explosions in the vicinity of control rooms," *Process Saf. Prog.*, **18**(1), 17–24, 1999.

[70] American Petroleum Institute, *Risk-Based Inspection Technology, API Recommended Practice 581*, 2nd ed. Washington, DC, USA: , 2008.

[71] Health and Safety Executive, "Failure Rate and Event Data for use within Risk Assessments," Health and Safety Executive, 2012.

[72] D. J. Finney, *Probit Analysis*, 3rd ed. Cambridge University Press, 1971.

[73] Y. H. Kim, "Optimal Layout of Chemical process using MILP & risk index approach," M.S. Thesis, Seoul National University, Seoul, Korea, 2011.

[74] H. Kim, K. Han, and E. S. Yoon, “Development of Dimethyl Ether Production Process Based on Biomass Gasification by Using Mixed-Integer Nonlinear Programming,” *J. Chem. Eng. Jpn.*, **43**(8), 671–681, 2010.

[75] T. A. Semelsberger, R. L. Borup, and H. L. Greene, “Dimethyl ether (DME) as an alternative fuel,” *J. Power Sources*, **156**(2), 497–511, 2006.

[76] DuPont, “Toxicity Summary for Dimethyl Ether (DME); Dymel® A Propellant,” 2011.

[77] Y.-H. Kim, W. So, D. Shin, and E. S. Yoon, “Safety distance analysis of dimethyl ether filling stations using a modified individual risk assessment method,” *Korean J. Chem. Eng.*, **28**(6), 1322–1330, 2011.

[78] K. Han, Y. H. Kim, N. Jang, H. Kim, D. Shin, and E. S. Yoon, “Risk Index Approach for the Optimal Layout of Chemical Processes Minimizing Risk to Humans,” *Ind. Eng. Chem. Res.*, **52**(22), 7274–7281, 2013.

[79] Korea Gas Safety Corporation, *Yearbook of Gas-related Accident*. 1987-2003.

[80] R. W. Prugh, “Plant Safety,” in *Kirk-Othmer Encyclopedia of Chemical Technology*, 3rd ed.**18**, New York: John Wiley, 1982.

[81] Brooke, A., Kendrick, D., Meeraus, A., and Raman, R., *GAMS - A User’s Guide*. Washington, DC: GAMS Development Corporation, 2012.

[82] S. Rebsdat and D. Mayer, “Ethylene Oxide,” in *Ullmann’s Encyclopedia of Industrial Chemistry*, Wiley-VCH Verlag GmbH & Co. KGaA, 2000.

[83] National Fire Protection Association, *NFPA 30: Flammable and Combustible Liquids Code*. National Fire Protection Association, 2012.

[84] U.S. Government Printing Office, *Protection of Environment*. 2008.

[85] F. I. Khan and M. R. Haddara, “Risk-based maintenance of ethylene oxide production facilities,” *J. Hazard. Mater.*, **108**(3), 147–159, 2004.

[86] N. Piccinini and G. Levy, “Ethylene oxide reactor: Safety according to operability analysis,” *Can. J. Chem. Eng.*, **62**(4), 547–558, 1984.

[87] W. So, “A Study on Design of Process Plant Layout based on Safety Assessment considering Domino Effect,” Ph.D. Thesis, Seoul National University, Seoul, Korea, 2012.

[88] Cathexis Consultancy Services Ltd., “Floating Production, Storage and Offloading (FPSO) Facilities,” presented at the Lillehammer Energy Claims Conference, 2012.

[89] Y. Gu and Y. Ju, “LNG-FPSO: Offshore LNG solution,” *Front. Energy Power Eng. China*, **2**(3), 249–255, 2008.

[90] W. H. Zhao, J. M. Yang, Z. Q. Hu, and Y. F. Wei, “Recent developments on the hydrodynamics of floating liquid natural gas (FLNG),” *Ocean Eng.*, **38**(14–15), 1555–1567, 2011.

[91] J.-H. Hwang, M.-I. Roh, and K.-Y. Lee, “Determination of the optimal operating conditions of the dual mixed refrigerant cycle for the LNG FPSO topside liquefaction process,” *Comput. Chem. Eng.*, **49**, 25–36, 2013.

[92] J.-C. Lee, J.-H. Cha, M.-I. Roh, J.-H. Hwang, and K.-Y. Lee, “Determination of the Optimal Operating Condition of Dual Mixed Refrigerant Cycle of LNG FPSO Topside Liquefaction Process,” *J. Soc. Nav. Arch. Korea*, **49**(1), 33–44, 2012.

[93] G. Venkatarathnam, “Natural gas liquefaction processes,” in *Cryogenic Mixed Refrigerant Processes*, K. D. Timmerhaus and C. Rizzuto, Eds. Springer New York, 2008, 149–220.

[94] S. Lee, N. V. D. Long, and M. Lee, “Design and Optimization of Natural Gas Liquefaction and Recovery Processes for Offshore Floating Liquefied Natural Gas Plants,” *Ind. Eng. Chem. Res.*, **51**(30), 10021–10030, 2012.

[95] J.-H. Hwang, N.-K. Ku, M.-I. Roh, and K.-Y. Lee, “Optimal Design of Liquefaction Cycles of Liquefied Natural Gas Floating, Production, Storage, and Offloading Unit Considering Optimal Synthesis,” *Ind. Eng. Chem. Res.*, **52**(15), 5341–5356, 2013.

[96] J.-H. Hwang, “Selection of Optimal Liquefaction Process System considering Offshore Module Layout for LNG FPSO at FEED stage,” Ph.D. Thesis, Seoul National University, Seoul, Korea, 2013.

[97] N.-K. Ku, J.-C. Lee, M.-I. Roh, and J.-H. Hwang, “Multi-floor Layout for the Liquefaction Process Systems of LNG FPSO Using the Optimization Technique,” *J. Soc. Nav. Arch. Korea*, **49**(1), 68–78, 2012.

초 록

지속 가능한 화학 공정 설계를 위한 리스크 기반의 배치 최적화에 관한 연구

본 논문은 화학 공정에서 발생 가능한 사고로부터의 개인적 리스크(Individual Risk, IR)를 정량적으로 평가하여 인명에게 미치는 영향을 제한할 수 있도록 하는 최적의 시설 배치 방법과 그 응용에 관한 연구이다. 화학 공정의 장치 및 설비는 운전 조건이 고온, 고압이거나 가연성, 유독성 등 위험 물질을 다루는데도 불구하고 비용 상의 문제로 인해 밀집된 형태로 공정이 구성되는 경우가 많다. 이로 인해 화재, 폭발, 독성가스 누출 등의 사고가 발생하여 인명 및 재산 피해 등을 야기할 가능성이 상존하며, 이에 대한 해당 공동체의 사회적 염려 또한 수반된다. 따라서 화학 공정의 지속 가능성을 확보하기 위해서는 장치 및 설비로부터 발생할 수 있는 리스크를 정량적으로 분석하여 이것이 실제 피해로 이어지지 않도록 하는 방안이 필요하다. 본

연구에서는 공정 설비의 배치를 조율하여 이러한 목표를 달성하고자 하였다.

먼저 공정 설비 배치 문제에 대한 기존의 다양한 접근법을 분석하고, 그 구성과 풀이 방법을 살펴보았다. 또한 화학 공정의 정량적 리스크 평가(Quantitative Risk Assessment, QRA) 방법과 리스크 지표에 대해 소개하였다.

이어서 지속 가능한 화학 공정 설계를 위한 리스크 기반의 설비 배치 최적화 문제를 정식화하였다. 공정과 관계된 작업자와 주변의 일반 시민이 화재나 폭발 사고로 인해 받을 수 있는 영향을 거리에 따른 개인적 리스크(IR)로 계산하고 이를 장치로부터의 안전 거리 기준으로 변환하였다. 얻어진 안전 거리를 기존의 배치 최적화 문제와 접목하여 장치 주변의 리스크 구역을 설정하는 문제로 구성하고, 부지, 배관, 장치 구입 및 방호 장치 설치 등 공정 건설에 필요한 비용을 최소화하여 경제적으로 최적화된 설비 배치를 제시하였다. 배치 문제의 구성은 혼합 정수 선형 계획법(Mixed-Integer Linear Programming, MILP)으로 이루어졌으며, 문제의 규모가 커질 경우에도 효율적인 풀이가 가능하도록 축소된 문제에 대한 반복적 탐색 방법을 활용하였다. 개인적 리스크(IR) 기반의 설비 배치 최적화를 통해 본질적 안전을 확보하면서도 경제적인 공정 배치를 이룰 수 있다.

제안된 배치 최적화 문제 방법은 세 가지 공정에 적용하여 그 타당성을 확인하였다. 첫 번째로, 가장 단순하지만 입지 특성 상 인명에 미치는 영향이 큰 연료 가스 충전소의 하나인 디메틸 에테르(Dimethyl ether, DME) 충전소의 설비 배치를 최적화하였다. 두 번째 대상 공정은 일반적인 규모의 화학 공정의 예시로서 산화 에틸렌(Ethylene oxide, EO) 생산 공정의 장치 배치 문제를 풀었으며, 공장 주변의 부지 이용 현황에 따른 간단한 입지 결정 문제를 다루었다. 마지막으로 보다 제한된 공간에서 다층으로 구성된 공정 배치 최적화의 사례로, 부유식 액화 천연 가스 생산/저장/하역 설비(Liquefied Natural Gas – Floating Production, Storage and Offloading vessel, LNG-FPSO)의 액화 공정을 다루었다. 이상의 사례 연구로부터, 제안된 방법이 화학 공정 설계 초기에 공정 배치의 안전성을 확보하여 공정의 지속 가능성을 높이고, 공정 배치와 관련된 의사 결정을 지원할 수 있음을 보였다.

주요어: 화학 공정 설계, 배치 최적화, 정량적 리스크 분석, 개인적 리스크.

학 번: 2007-21234